Journal of Solar Energy Engineering. Received August 06, 2018;
Accepted manuscript posted December 10, 2018. doi:10.1115/1.4042203

Solar and climatic high performance factors for the placement of solar power plants in Argentina Andes sites. Comparison with African and Asian sites.

Della Ceca L.S[1], Micheletti M.I[1,2], Freire M.[1], Garcia B.[3], Mancilla A.[3], Salum G.M.[4], Crinó E.[5] and Piacentini R.D[1,6]

1. Instituto de Física Rosario (CONICET – Universidad Nacional de Rosario), Rosario, Argentina
2. Facultad de Ciencias Bioquímicas y Farmacéuticas, Universidad Nacional de Rosario, Rosario, Argentina
3. Instituto de Tecnologías en Detección y Astropartículas, Universidad Tecnológica Nacional, Facultad Regional Mendoza, Mendoza, Argentina
4. School of Biological Sciences and Engineering, Yachay Tech University, Urcuquí, Ecuador
5. Facultad de Ciencias Fisico-Matemáticas y Naturales, Universidad Nacional de San Luis, San Luis, Argentina
6. Laboratorio de Eficiencia Energética, Sustentabilidad y Cambio Climático, IMAE, Facultad de Ciencias Exactas, Ingeniería y Agrimensura, Universidad Nacional de Rosario, Rosario, Argentina.

Corresponding authors: Della Ceca, Lara Sofía dellaceca@ifir-conicet.gov.ar/dellaceca.lara@gmail.com or Rubén D. Piacentini, ruben.piacentini@gmail.com. Instituto de Física Rosario (CONICET – Universidad Nacional de Rosario), Bv 27 de Febrero 210 bis, 2000, Rosario, Argentina.

Highlights

- Solar and climatic factors are analysed in Puna of Atacama desert, Argentina
- Argentinean Andes range have sites that are very well suited for PV power plants
- African (Ouarzazate) and Asian (Dubai) sites are analysed for comparison purposes

Abstract

The installation of solar power plants is currently having a notable expansion. The results presented show that the Argentinean Andes range, from the central to northern latitudes, is an excellent region for the placement of these plants, due to the sum of different positive factors: very high mean annual solar irradiation, low ambient temperature and relative humidity, low precipitable water content, normal wind speeds and extremely low aerosol content of the atmosphere. The proposed regions are nearby San Antonio de los Cobres and El Leoncito, and are compared with two important locations where large solar power plants have been (or will be) built: a site in Africa (Ouarzazate, Morocco) and one in Asia (Dubai, Arab Emirates). We present results of the possible production of electricity, supplying a total of about 21000 GWh, which is 15.6% of the 2015 Argentinean electric consumption and, consequently, could reduce the

emission of greenhouse gases in a total mass of 11.2 million tons of CO_2eq. The installation of this type of renewable power plants, will contribute significantly to the Argentinean population due to frequent (mainly summer) cutoff of electric power supply and, in particular, to isolated (low income) populations leaving in the Argentinean Andes range.

Keywords: Solar radiation, Climatic data, Solar power plant, Andes, Argentina

1. Introduction

A large fraction of the full energy matrix employed worldwide consists of fossil fuels. In 2015, the International Energy Agency estimated that this fraction was 81.5% [1]. In Argentina, the dependence on fossil fuels is even larger: 87% of the total amount in 2016 [2]. Renewable energy is having at present a notable expansion, also expected for the near future. In 2015, the National Congress of Argentina approved a Law (Law Number 27191) for the promotion of renewable energies in the framework of a national plan to achieve a 20% of renewable energy use at the end of 2025. The main arguments for the introduction of clean energy sources are the reduction of the dependence on imported fossil fuels and in installation costs with respect to conventional sources, mitigation of the emission to the atmosphere of GHG responsible of the global warming [3] and, additionally, the access to electricity for people living far apart from important electric sources (thus providing a platform for their human development).

In the last decades, in the field of photovoltaic solar energy (PV), important efforts have been made in technological research to reduce manufacturing costs and obtain greater efficiencies [4-5].The selection of sites to place solar PV power plants is a critical issue because large investments are required by companies and/or governments.

The knowledge of the solar radiation in a particular location is of basic importance for the decision to install solar power plants. The Puna of Atacama desert in the North-West Argentina Andes range is one of the regions of the world with the highest solar irradiance values, as was shown by Piacentini et al [6]. A confirmation that the Central East Andes region has high values of incident solar radiation is given, for example, by the Global solar atlas published on line by the International Renewable Energy Agency, IRENA [7].

In addition, other variables that may affect the behavior of a solar power plant should be taken into account when studying a site for the placement of a solar power plant. For example, the knowledge of the daily cloud coverage is important for its contribution to the reduction of the solar irradiation availability, and also for the problems that can be produced by the shadow of dense clouds that arrive on the solar PV power plan. An unbalance in the photovoltaic current can affect the behavior of the modules at shadow, with respect to the other ones [8].

Temperature is another factor of importance in the definition of a solar PV power plant, since the quantum cell efficiency, which measures the possibility to capture solar photons to produce electricity, is temperature dependent. In particular, the most common cell material is based on crystalline Silicon and has a dependence of around 0.4 % per ºC (see for example, [9]). Consequently, sites that have a lower mean annual ambient temperature and use this type of cells will be more efficient than others with higher temperatures.

The relative humidity is one of the factors that affect materials exposed to outdoor commonly used in solar power plants, like iron, through oxidation.

Precipitable water also influences solar radiation, since the solar irradiance in the IR range is reduced with the increases of the water content of the atmosphere.

Moreover, the microscopic particulate matter (or aerosols) content of the atmosphere play significant roles in the attenuation of solar radiation incident on the collection plane: a) when they are present in atmospheric suspension, they scatter and absorb solar photons (depending on the particle type, the latter mainly related with black carbon) and b) when they are deposited on the PV panels (see for example, [10]). For instance, in the 7 MW concentrated solar power plant at Mirrah Solar Thermal Project, Oman, to avoid the desert sand deposition on the parabolic mirrors, a glass greenhouse was built to protect them [11].

Actually in Argentina, an experimental solar PV power plant of about 1.1 MW peak installed in Ullum, Province of San Juan is producing electricity [12] and one of the largest solar PV power plants of Latin America of 300 MW peak was recently built (2017) in the Puna of Atacama desert, in Cauchari, Department of Susques, Province of Jujuy. However, there are very few studies that evaluate how propitious a site is for the generation of solar energy or other type of renewable energy in Argentina [6, 13].

The aim of this study is to evaluate climatic (ambient air temperature, relative humidity, winds, precipitation), atmospheric particles (aerosol concentration, aerosol optical depth) and solar radiation conditions at two sites (San Antonio de los Cobres and El Leoncito, and their surrounding area) in the Argentinean (East) Andes range, where large PV (and photo thermal) solar power plants can be emplaced. We compare these sites with others selected in other continents for solar energy generation: Ouarzazate, Morocco, in Africa, where a large solar plan is operating, and Dubai, United Arab Emirates, in Asia, where a large solar plant is currently under construction. We show in this work that the mentioned Argentinean sites present better solar and climatic conditions for the installation of solar facilities installed there. In addition, we present an estimation of the amount of energy that an installed plant could produce in these Argentina Andes range sites.

2. Materials and Methods

2.1 Study area

The geographical location of the two rather flat sites (surrounded by mountains) in the Argentina Andes range: San Antonio de los Cobres (Province of Salta) and El Leoncito, in the Pampa El Leoncito (Province of San Juan) is detailed in Figure 1.

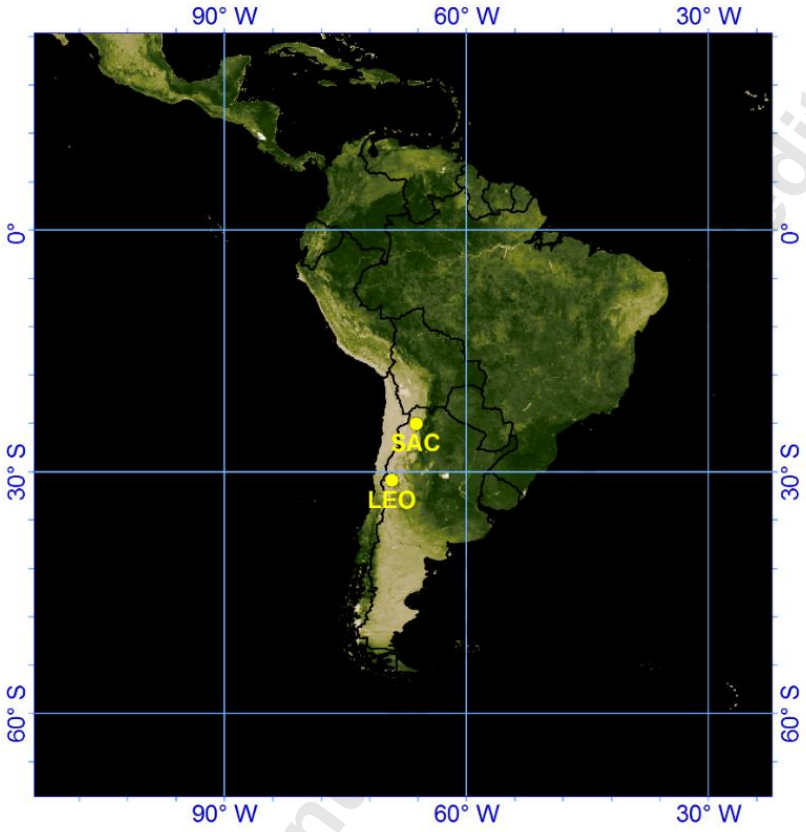

Figure 1. Map of South America showing the geographic location of the two sites proposed for the placement of solar power plants in Argentina: San Antonio de los Cobres (SAC, *24.045°S, 66.235°W, 3607 m a.s.l*) and El Leoncito (LEO, *31.08 °S, 69.27 °W, 2627 m a.s.l*). Image source: Normalized difference vegetation index (NDVI) MODIS/Terra product, Goodard Space Flight Center/NASA at https://neo.sci.gsfc.nasa.gov.

2.1.1 San Antonio de los Cobres site

San Antonio de los Cobres site (SAC) is located in the Atacama Desert, called *Puna* in Argentina (the largest high altitude desert in the world), with a mean altitude value in the 3500-4000 m a.s.l range and with mountain peaks with altitudes in the 6000-6500 m a.s.l range.

Figure 2 shows geographical characteristics of the SAC site and the surrounding flat region. As it can be observed, this area corresponds to a rather large surface (59.8 Km^2) with a mean North-South distance of 16.6 Km and a mean East-West distance of 5.4 Km, with a mean altitude of 3607 m a.s.l (Figure 2.Top). Moreover, as shown by the slope curves displayed in Figure 2.Bottom, the area has a rather small slope, with a mean value of *(91 ± 47) m/Km.*

Journal of Solar Energy Engineering. Received August 06, 2018;
Accepted manuscript posted December 10, 2018. doi:10.1115/1.4042203

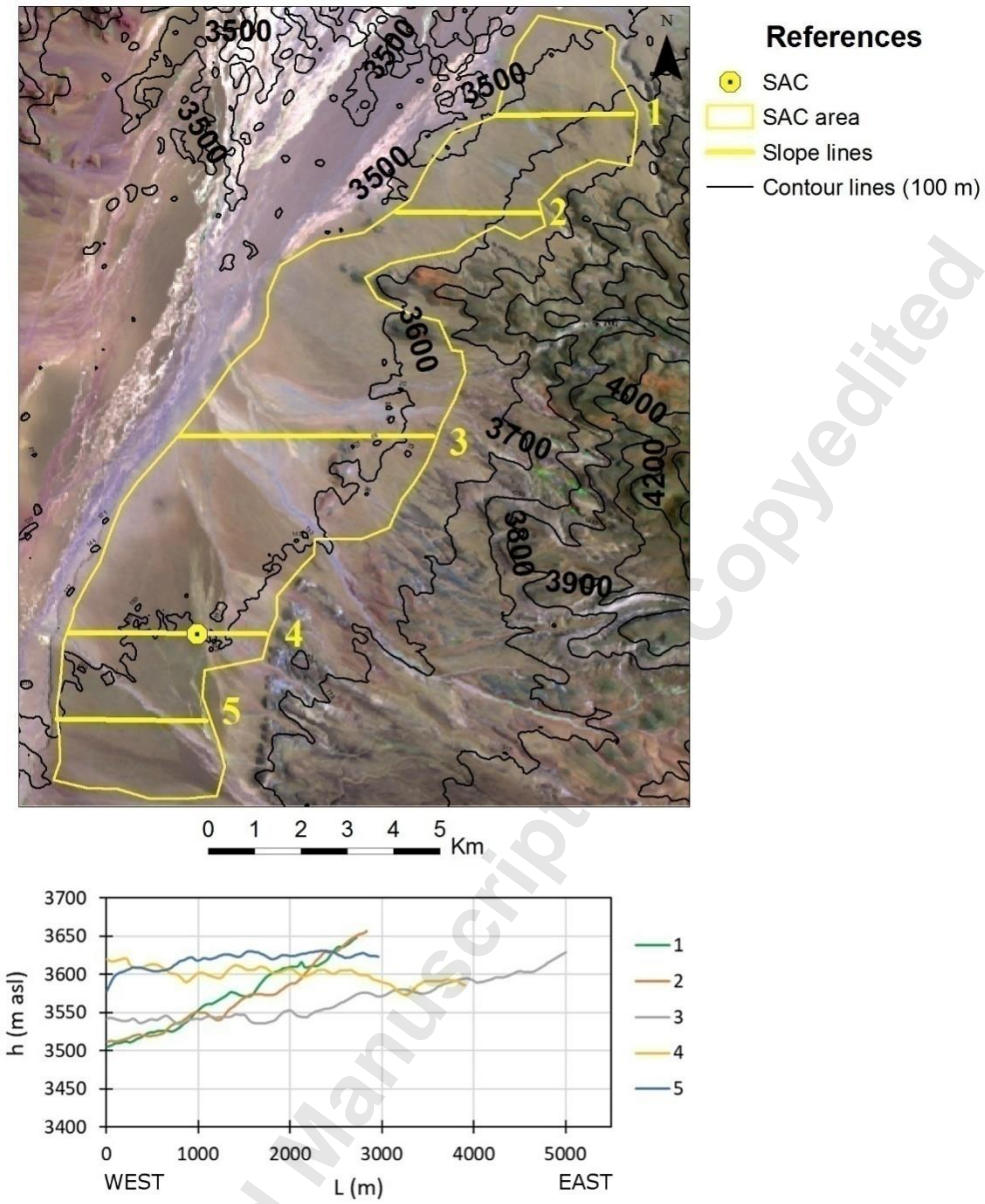

Figure 2. Top. Location of the San Antonio de los Cobres (SAC) (yellow circle) and nearby region at the Puna of Atacama desert, in Argentina Andes range with indication of the isolines (lines in black). The black numbers are altitudes in meters, the straight yellow lines indicate the places where the slopes are calculated (see bottom figure) and the yellow curve indicates the proposed limit for the placement zone of the solar power systems. Bottom: altitudinal data as function of distance from the West point of the sites, where slope lines numbers 1 to 5 are indicated in the top figure. Source of top figure: Landsat 8 obtained 16/08/2016, band combination RGB: 432 (source: US Geological Survey).

2.1.2 El Leoncito site

El Leoncito (LEO) Astronomical Observatory Complex is located at the Pampa El Leoncito (Figure 3). LEO site and its flat surrounding area have an approximately area of 151 Km^2 (at a mean height of 2627 m a.s.l), with a mean North-South distance of *24.4 Km* and a mean East-West distance of *7.3 Km*, larger than the

described SAC area. In this Central Argentina Andes range, the LEO region has inclinations with a mean value of *(361±46) m/Km* (Figure 3.Bottom).

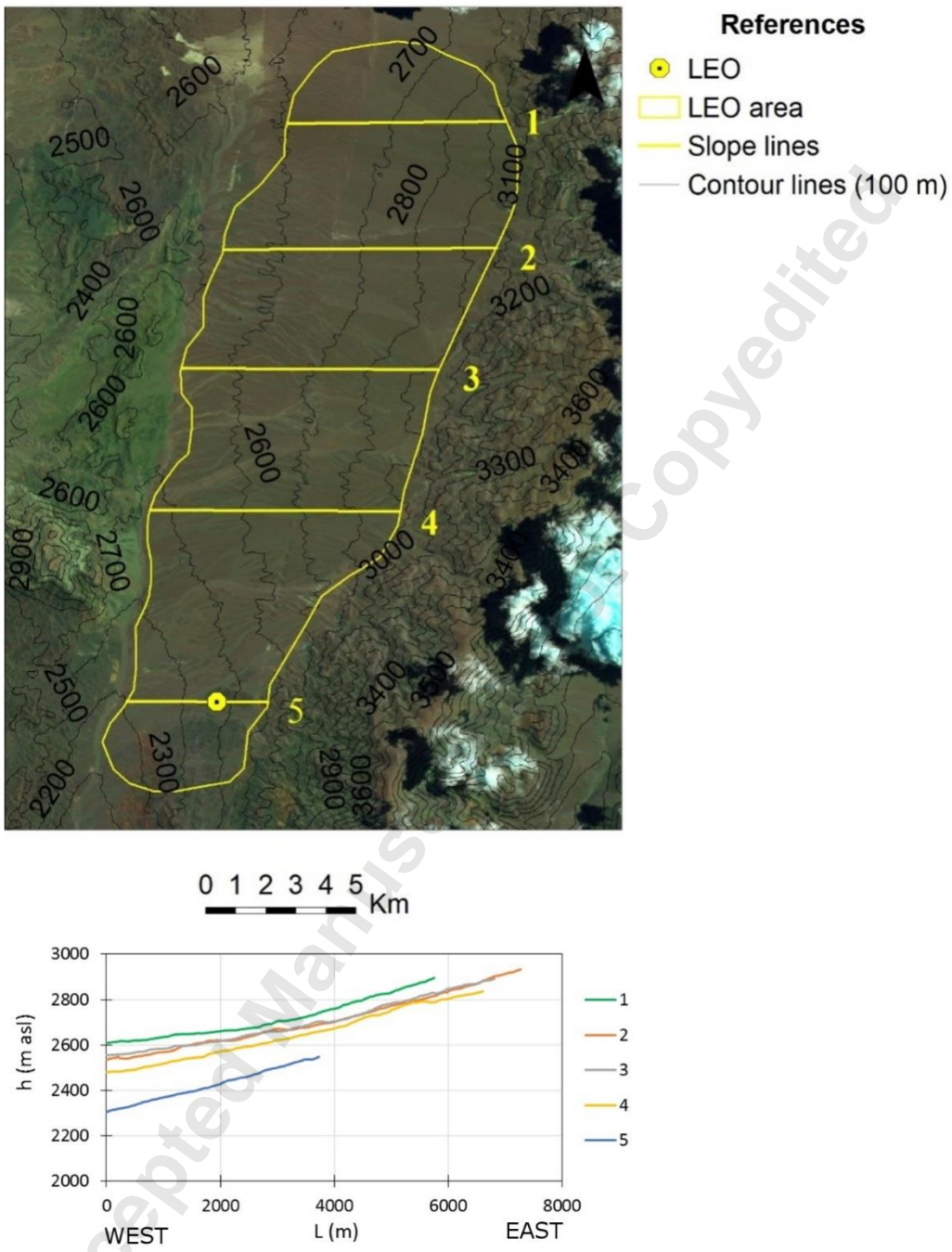

Figure 3. Top. Location of the El Leoncito (LEO) site (yellow circle) and nearby region at the Central Argentina Andes range with indication of the isolines (lines in black). The black numbers are altitudes in meters, the straight yellow lines indicate the places where the slopes are calculated (see bottom figure) and the yellow curve indicates the proposed limit for the placement zone of the solar power systems. Bottom: altitudinal data as function of distance from the West point, of the sites where slope lines numbers 1 to 5 are indicated in the top figure. Source of top figure: same as Figure 2.

2.2 Solar radiation, meteorologic and atmospheric variables considered in this study

In a previous study carried out for the selection of possible sites for the placement of a new generation of the astrophysical Cherenkov Telescope Array in the Southern Hemisphere [14], we analyzed in detail two sites of the Argentina (East) Andes range: San Antonio de los Cobres and El Leoncito sites. In this previous work, with a definite orientation in the placement of an Astrophysical observatory for the detection of ultra-energetic gamma photons in the range of *GeV* (Giga electron volt) or even *TeV* (Tera electron volt) energy ranges, we presented mainly results for the *night periods*. In the present work, we will consider mainly data *for the hours of the day with solar radiation*, since we are interested in the placement of solar power plants. We also extend the analysis to new variables of interest for this type of power plants. It must be pointed out that these plants will not interfere with astronomical/astrophysical observations, if they are placed in the same proposed sites by taking into account sustainability criteria, like the LEED (Leadership in Energy and Environmental Design) ones [15], as a very clean construction and maintenance process. On the other hand, interference would occur if conventional (fossil fuel) power plants were considered for the placement, due to the emission to the atmosphere of contaminant gases and aerosols.

The variables considered in this study that can influence the behavior of a solar power plant, and their measurement methods, are described below.

2.2.1 Solar radiation

Daily solar irradiation incident on a horizontal plane and daily solar irradiation incident on the optimum near latitude inclined angle were obtained from the Surface Meteorology and Solar Energy (SSE)/NASA database (available at: https://eosweb.larc.nasa.gov/).

The SSE/NASA project, from which we obtained the solar radiation and meteorological data used in our study, was initially released more than two decades ago (in 1997) by the Applied Science Program of NASA's data holdings. The SSE data-delivery website has as purpose to provide easy access to important parameters for renewable energy sources. This database is continuously updated. In addition, estimates of data uncertainty are made based on comparisons with surface measurements around the world. A detailed description of the parameters and the procedures used to estimate their uncertainties can be found in (https://power.larc.nasa.gov/documents/POWER_Data_v8_methodology.pdf; [16-18]). It has been shown that these satellite and model-based products are accurate enough to provide reliable data on solar and meteorological resources in regions where surface measurements are scarce or non-existent. Meteorological variables present a Mean Bias Error (MBE) in the range -8.59 to 4.44% and a Root Mean Square Error (RMSE) in the range 1.05 to 24.05% over the comparison years. In addition, these products offer two unique characteristics: the data are global (allowing the comparison of different sites) and, in general, present continuity over time.

It is important to remark that the measurements were made by similar satellite (well calibrated) instruments and for the same period of 22 years: July1983 - June 2005.

Direct solar radiation can be used as a test for the determination of the solar transmittance of the atmosphere. We employed the SMARTS2 algorithm developed by Gueymard [19] to determine the direct spectral solar irradiance at both, SAC and LEO sites, by considering a vertical path and typical values for atmospheric variables (Table 1). A study of the (good) accuracy of this SMARTS2 broadband radiative model with respect to other 17 models was analyzed by Gueymard [20].

The spectral solar transmittance was determined from the ratio of the spectral direct solar irradiance at ground with respect to the extraterrestrial one (at each wavelength).

Table 1. Atmospheric components and solar constant parameters, considered for the calculation of the (UV and Visible) photon transmittance presented in Figures 6, employing the SMARTS2 algorithm [19].

Parameter	SAC site	LEO site
Ozone (DU)	249	278
Aerosol (AOD_{550})	0.024	0.027
Water content (cm)	0.53	0.73
CO_2 (ppm)	398.8	398.8
Atmosphere kind	Desert	Desert
Albedo	0.06	0.06
Solar constant (W/m^2)	1361.3	1361.3

2.2.2 Meteorological data

The ground data acquisition was performed using a Reinhardt MWS 4M weather station [21], located at 3 meters over the ground level and connected to a single board computer. These data (for SAC from September 2012 to October 2013, and for LEO from January 2012 to September 2014) were stored at the device in a convenient ad-hoc format. The ground meteorological data (temperature, relative humidity, winds) were acquired every 1 minute, being then averaged over a 10 minutes period before the daily analysis. The results corresponding mainly to the daylight period, between *6:00* and *20:00 hours*, local time (= UT – 3 hours) in the September 2012 – August 2013 period, are presented in sections 3.1.4, 3.1.5 and 3.1.6. For the statistical analysis of the measured variables, we employed at each of the x-axis values, the *normal distribution function* $f(x,\mu,\sigma)$, where μ is the mean value and σ the standard deviation.

We also analyzed satellite data, in order to establish a comparison with other sites and to have data from another source in the case of no ground-based results. In particular, medium air temperature at 10 meters above the ground surface, relative humidity, precipitable water and wind speed were obtained from the SSE/NASA database.

2.2.3 Cloud fraction

The cloud fraction in SAC and LEO was studied in the framework of the characterization of these sites for the Cherenkov Telescope Array (CTA) project, using an All Sky Camera (ASC) hardware and the

corresponding software, as a universal device for the monitoring of the night sky quality (see [22]). The percentage of cloud coverage presented in this work corresponds to measurements made between 8 pm and 6 am, from September 2012 to October 2013 at SAC, and from January 2012 to September 2014 at LEO. When measured with a satellite instrument, the cloud fraction is the ratio between the attenuated cloud satellite sensor pixel counts, divided by the total pixel counts. For this study, daylight cloud amount was also obtained from the SSE/NASA database.

2.2.4 Particulate matter concentration

For ground-based measurements, we used a GRIMM aerosol spectrometer model 1.109. This is a portable device designed for continuous measurements of airborne aerosol concentration in two possible modes: particle concentration (particles/liter) or mass concentration (µg/m3). Concentrations are obtained in size intervals, for particles with diameter >0.22 µm, thus giving the aerosol size distribution. The measuring principle of this instrument is based on the detection of the single-particle scattering of the light emitted by a laser diode, thus allowing the classification of the signals to the corresponding different particle sizes (Figure 4).

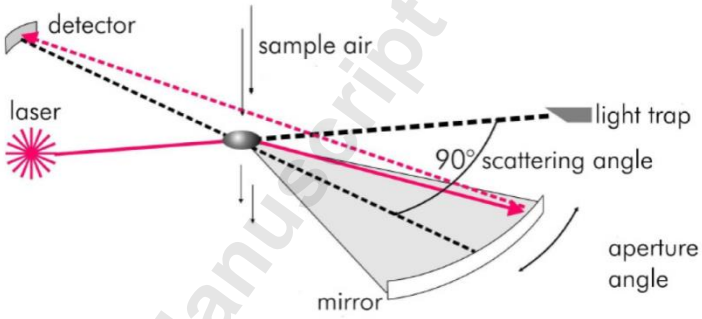

Figure 4. Grimm 1109 principle of operation. Source: Grimm, Tchenik GmbH & Co, Portable Laser Aerosol spectrometer and dust monitor 1.108/1.109 User manual, page 11 [23].

Samples of the ambient air containing the suspended particles are continuously led into the measuring cell at a constant flow rate (*1.2 liter/minute*). A λ*=655 nm* laser diode is used as a light source. Every particle crossing the light beam generates a scattering pulse. The number of signals detected gives the number of particles, while the intensity of these scattering signals is related to a certain particle size. Using a wide opening angle mirror to reflect scattering light onto the light detector, it is possible to classify the particles in 31 size intervals (channels) within the size range *0.25 µm – 32.0µm*. Depending on the operation mode selected, the GRIMM aerosol spectrometer can determine particle or mass concentration for each size channel. Finally, aerosols are collected in a gravimetric polytetrafluoroethylene (PTFE) filter (47 mm, 0.2 µm nominal pore size) for further analysis.

Even if GRIMM 1.109 cannot measure in both modes directly, it is possible to calculate number concentration per channel from mass concentration measurements (Mathias Barthel GRIMM Company, private communication). To do this, is necessary to assume spherical particles and the mass density of aerosols. Grimm measurements were obtained every one minute at 2.5 m above ground, at both sites LEO and SAC. The data was taken during the following periods of time (initial and final times are expressed using local time, *UTC -3 hours* for Argentina): for LEO site from 27th December 2012 (*4:10 am*) to 4th January 2013 (*5:35 pm*) and for SAC from 6th May 2013 (*3:32 pm*) to 9th May 2013 (*3:31 pm*).

To define daytime and nighttime for concentration analysis, the NOAA solar calculator was used [24], for each measurement campaign. This algorithm calculates the apparent sunset/sunrise of a certain position and date (input data required are latitude/longitude, year, month and day), making corrections due to atmospheric refraction. Although atmospheric conditions can introduce errors of several minutes on the results, in this paper the apparent sunset/sunrise is used only as a way to distinguish daytime from nighttime. Since the measurements on each site last a few days, a single local hour value for sunrise and a single one for sunset has been considered: *8:00 am* and *9:00 pm* for SAC, *7:00 am* and *10:30 pm* for LEO. The sunrise and sunset times were chosen as a rounded value near the mean apparent sunrise/sunset time for each day of measurement, at each site.

2.2.5 Aerosol Optical Depth

The Aerosol Optical Depth (AOD) is a dimensionless parameter that indicates the content of aerosols (e.g., urban haze, smoke particles, desert dust, sea salt) distributed within a column of air from the Earth's surface to the top of the atmosphere. The total optical depth (τ_{TOT}) can be obtained, considering the Beer-Lambert-Bouguer law, using the following equation:

$$I(\lambda) = Io(\lambda)\, d^2\, exp[-\tau_{TOT}(\lambda)\ m] \quad (1)$$

where I is the spectral irradiance measured at wavelength λ, Io is the top of the atmosphere spectral irradiance, d is the ratio of the average to the actual Earth-Sun distance, τ_{TOT} is the total optical depth, and m is the optical air mass [21]. The optical depth due to other atmospheric components (water vapor, Rayleigh scattering, and other wavelength-dependent trace gases) are then subtracted from the total optical depth to obtain the aerosol component:

$$\tau_{Aerosol}(\lambda) = \tau_{TOT}(\lambda) - \tau_{water}(\lambda) - \tau_{Rayleigh}(\lambda) - \tau_{O3}(\lambda) - \tau_{NO2}(\lambda) - \tau_{CO2}(\lambda) - \tau_{CH4}(\lambda) \quad (2)$$

AOD ranges from near 0 (low content) to ≥ 5 (high content of aerosols).In this study we used the AOD measured by the SeaWiFS instrument on board the SeaStar/NASA satellite [26] at *550 nm* and, when available, by ground-based sun photometers. Data was obtained from the NASA web application [27].

AOD ground-based measurements were also carried out by a Cimel sun photometer at the CASLEO station (*69.30 ºW 31.79 ºS*) of the AERONET/NASA network (https://aeronet.gsfc.nasa.gov) in the 2011-2013

period. The AERONET (Aerosol Robotic NETwork) project is a federation of ground-based remote sensing aerosol networks established by NASA and PHOTONS (PHOtométrie pour le Traitement Opérationnel de Normalisation Satellitaire) which provide long-term, continuous and public domain database of aerosol optical, microphysical and radiative properties for aerosol research and characterization, for validation of satellite retrievals.

Results and Discussion

3.1 Solar radiation and atmospheric variables

This section includes the results of the variables measured at LEO and SAC sites and obtained from satellite sensors in order to compare with an African site (Ouarzazate, Morocco, *30.934°N; 6.937 °W, 1137 m a.s.l*) and an Asian one (Dubai, United Arab Emirates*24.755°N; 55.365°E, 113 m a.s.l*) site, in which large solar power plants are (or will be) placed. In the first case, the Noor Ouarzazate Solar Complex "forms part of the Moroccan Solar Energy Program, which aims to develop five solar complexes with a combined capacity of approximately *2 GW* by 2020 to meet the energy demands of the country, which depends on *95%* imports" [28]. In the second case, the *800 MW* Mohammed bin Rashid Al Maktoum Solar Park, near Dubai, will be completed in 2020; additionally, an extension of this Complex of three solar PV plants is expected to arrive at *5000 MW* by 2030 [29].

3.1.1 Solar global radiation

Figure 5.Top shows the monthly mean of daily solar irradiation incident on a horizontal surface at SAC and LEO sites. The observed opposite behavior of this variable throughout the months of the year on LEO and SAC with respect to Ouarzazate and Dubai sites is simply due to the fact that they are located in different hemispheres, the Southern one and the Northern one, respectively. The annual mean of daily solar irradiation on the horizontal plane at the four sites (Figure 5.Bottom) has increasing values in the order SAC > LEO ~ Dubai > Ouarzazate.

However, what is more important than the solar radiation incident on a horizontal surface is the solar radiation incident on the optimum (near latitude) inclined angle given in Figure 6.Top. For this variable, the solar irradiation in SAC and Dubai (sites at similar absolute latitudes, *24.05 °S* and *24.75 °N*, respectively, even if in different hemispheres) increases with respect to the horizontal plane of incidence, in a quite similar proportion: *5.8%* and *3.4%*, respectively. A similar behavior but with an even larger increase due to the fact that their latitudes are higher, is observed for LEO and Ouarzazate (placed at *31.08 °S* and *30.93 °N*, respectively). Their corresponding proportions increase: *7.6%* and *8.5%*, respectively.

Journal of Solar Energy Engineering. Received August 06, 2018;
Accepted manuscript posted December 10, 2018. doi:10.1115/1.4042203

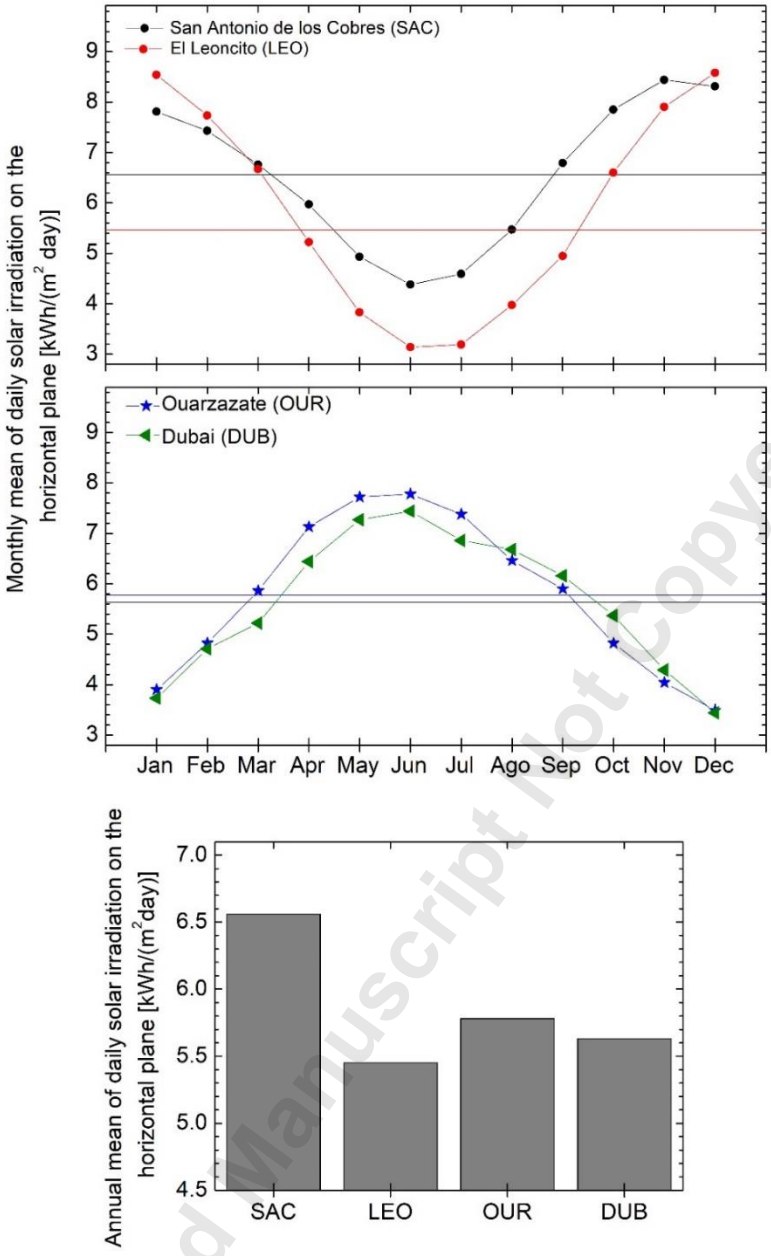

Figure 5. Top. Monthly mean of daily solar irradiation incident on a horizontal plane in the four investigated places: the high altitude Argentinean sites of SAC and LEO, the Sahara desert African site of Ouarzazate (OUR), Morocco and the Arabic desert near Dubai site (DUB). The annual mean is also given as a horizontal line of the same color as the corresponding curve. Source of data: SSE/NASA. Bottom: The annual mean of each curve is represented by a vertical gray bar, for the four different places, for comparison purposes.

Journal of Solar Energy Engineering. Received August 06, 2018;
Accepted manuscript posted December 10, 2018. doi:10.1115/1.4042203

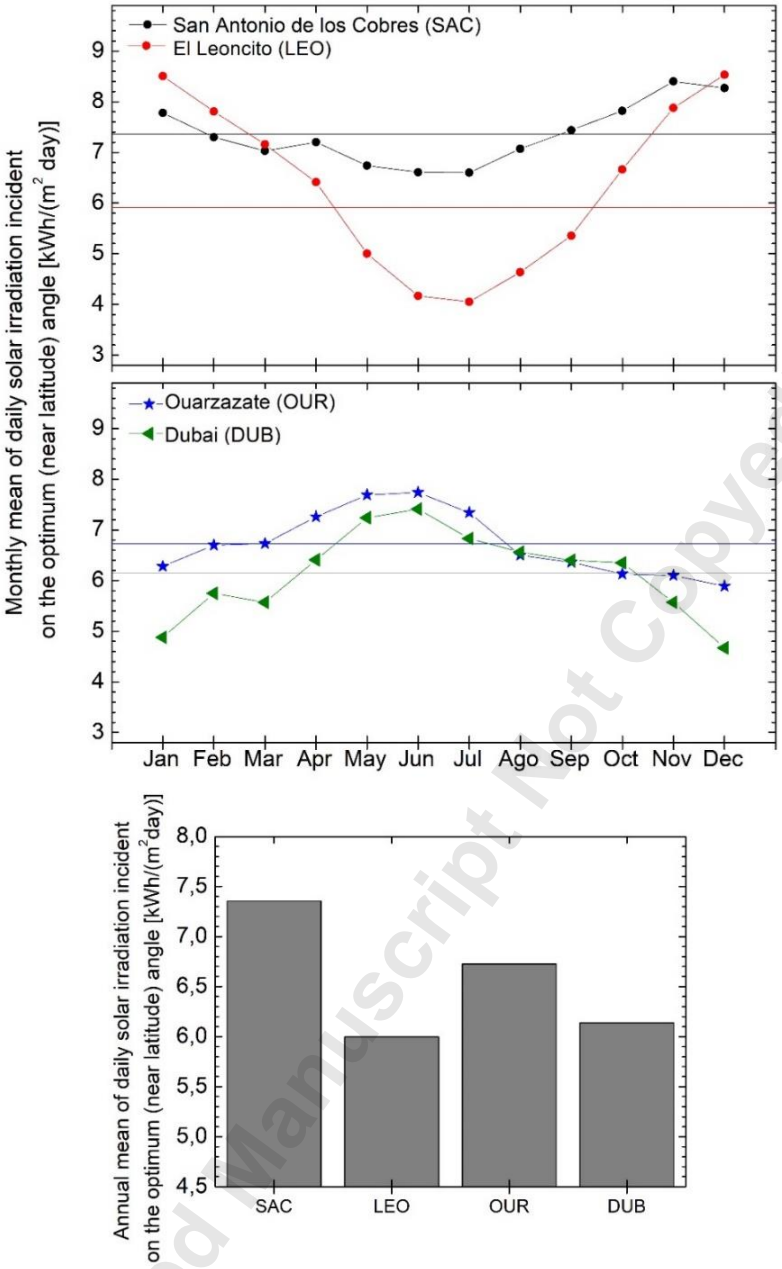

Figure 6.Top. Monthly mean of daily solar irradiation incident on the optimum (near latitude) angle of the site in the four investigated places, represented in a similar way as in Figure 5.Top. Source of data: SSE/NASA. Bottom: The same as in Figure 5.Bottom, for the annual mean of solar irradiation incident on the optimum (near latitude) angle.

3.1.2 Atmospheric transmittance to direct solar radiation

Results of the *direct solar radiation transmittance* of the atmosphere, obtained by employing the SMARTS2 algorithm (see item 2.2.1), at SAC and LEO sites are shown in Figure 7. As expected from the higher altitude (since the aerosol content is quite similar), the SAC solar transmittance is higher (and significant) at all wavelength than the solar transmittance at LEO, mainly due to the near 1Km difference in altitude with an atmosphere that varies approximately exponentially.

Journal of Solar Energy Engineering. Received August 06, 2018;
Accepted manuscript posted December 10, 2018. doi:10.1115/1.4042203

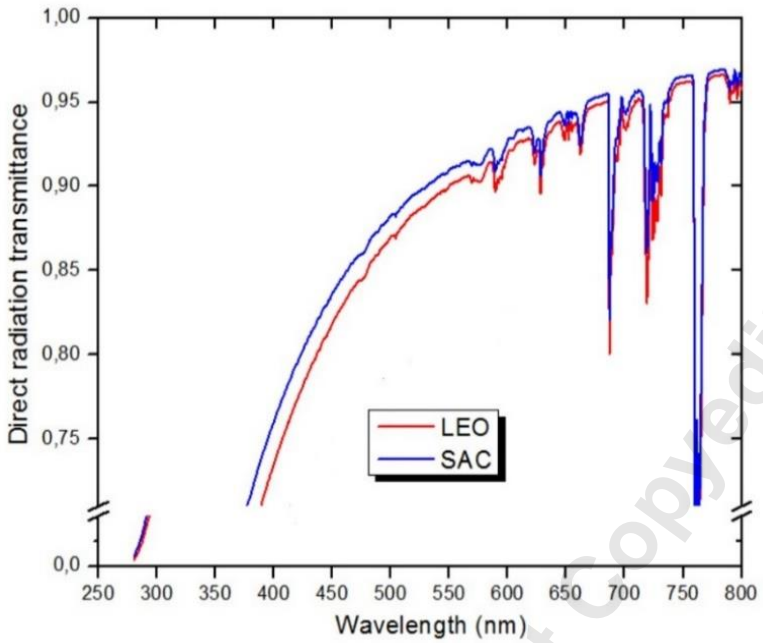

Figure 7. Direct solar radiation transmittance along a vertical path through the atmosphere of the Argentinean East Andes range sites of SAC and LEO, calculated employing the SMARTS2 algorithm [16].

3.1.3 Cloud fraction

The measurements of night cloud fraction at SAC and LEO sites were published by Piacentini et al [12]. These results indicate that more than *85%* of the measurement time was considered as clear sky nights for SAC and over *78%* for CASLEO, showing the good quality of these skies, when cloud fraction is concerned, for astrophysical/astronomical applications.

In Figure 8.Top, we represent the monthly mean of the daylight cloud amount percentage in the four investigated places. The highest value corresponds to LEO (57.3%), followed by SAC (37.4%), Ouarzazate (33.3%) and Dubai (30.3%), as displayed in Figure 8.Bottom. The maximum dispersion of the cloud fraction corresponds to Dubai site, varying in the range of 16% to 50% and to the LEO site, in the range of 40% to 70%. The possible higher values of SAC and LEO with respect to OUR and DUB could be due to the difficulty for the satellite data in the separation of cloud reflectivity from that of other sources like snow and salt surfaces (the last one usually of ancient lakes).

Journal of Solar Energy Engineering. Received August 06, 2018;
Accepted manuscript posted December 10, 2018. doi:10.1115/1.4042203

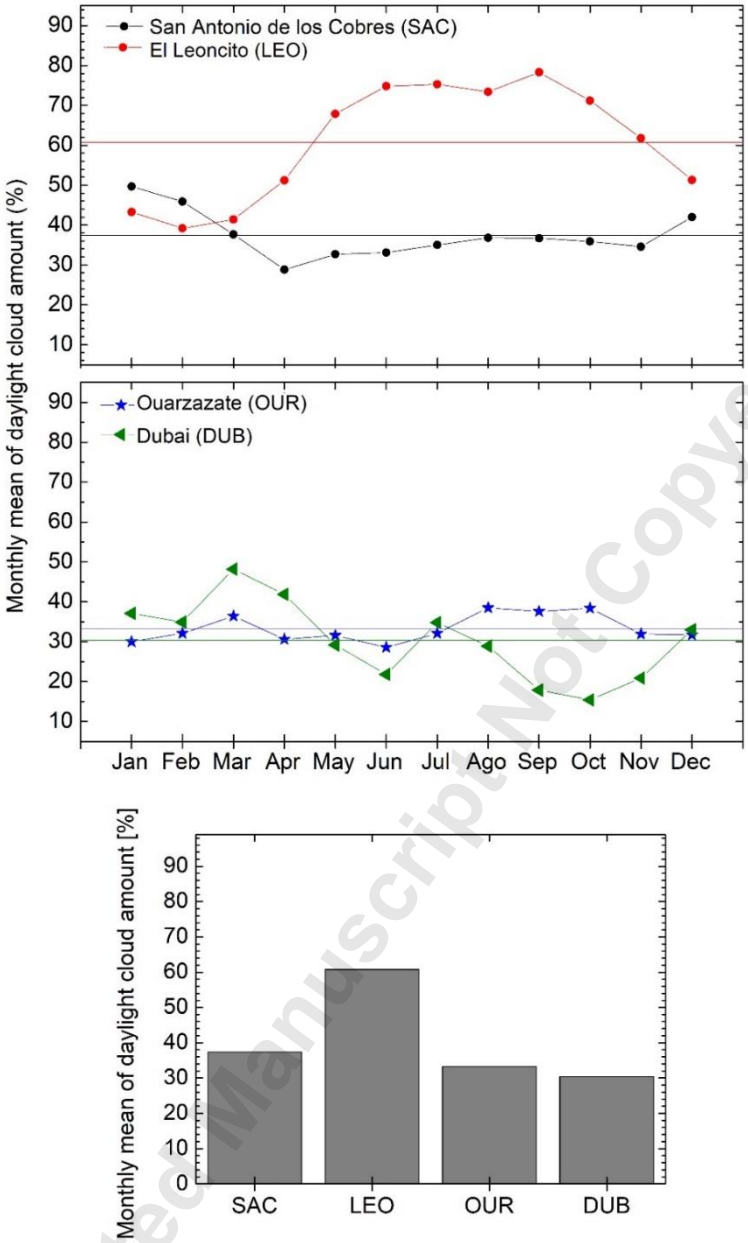

Figure 8.Top: Percentage monthly mean of daylight cloud amount in the four investigated places, represented in a similar way as in Figure 5.Top Source of data: SSE/NASA. Bottom: The same as in Figure 4.Bottom, for the annual mean of daylight cloud amount.

3.1.4 Ambient (air) temperature

The daily maximum, average and minimum ambient temperatures measured by the Reinhardt MWS 4M weather station are displayed as a function of time in Figures 9 and 11 for SAC and LEO sites, respectively. The probability densities for these sites are presented in Figures 10 and 12. From a statistical analysis that employs the normal distribution function, we determined the average temperature and standard deviation for each site, being (13.0 ± 6.9) ºC for SAC and (13.5± 6.8) ºC for LEO.

Journal of Solar Energy Engineering. Received August 06, 2018;
Accepted manuscript posted December 10, 2018. doi:10.1115/1.4042203

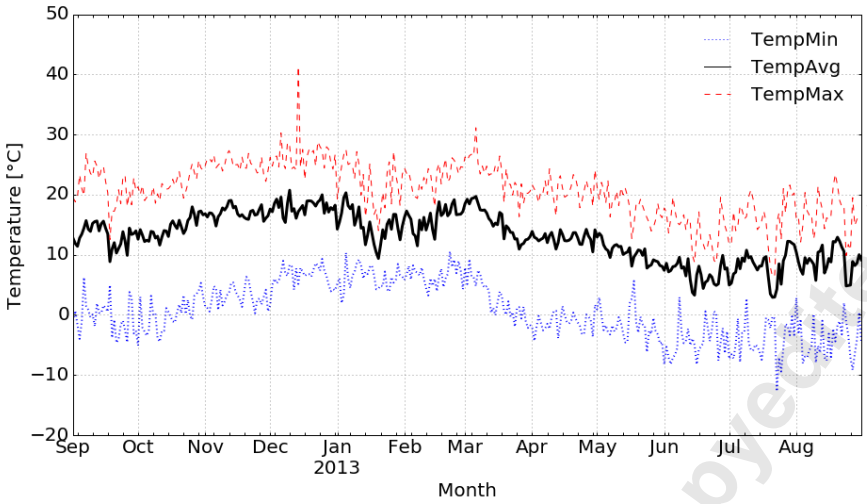

Figure 9. Temporal series of (maximum, mean and minimum) ambient temperature (°C) at SAC site. The data were obtained during the day, between 6:00 and 20:00 hours, local time (= UT – 3 hours) in the September 2012 – August 2013 period, employing the Reinhardt MWS 4M weather station.

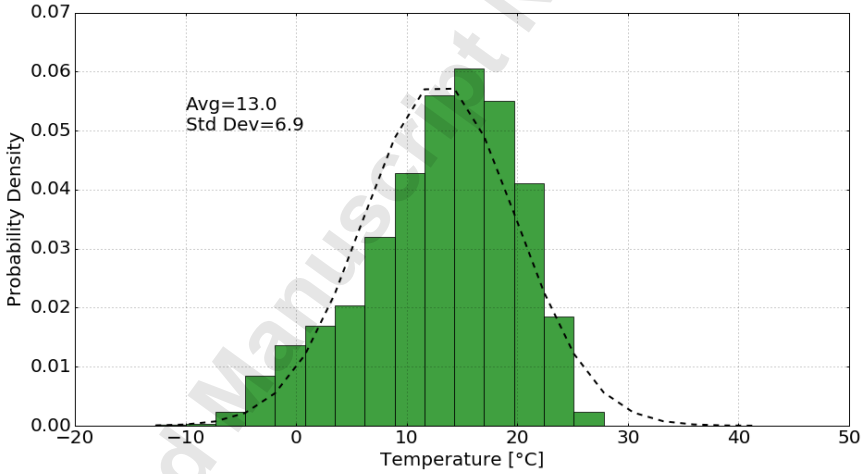

Figure 10. Ambient temperature probability density at SAC site, obtained through a statistical analysis of the data displayed in Figure 9. The broken curve is the corresponding *normal distribution function.*

Journal of Solar Energy Engineering. Received August 06, 2018;
Accepted manuscript posted December 10, 2018. doi:10.1115/1.4042203

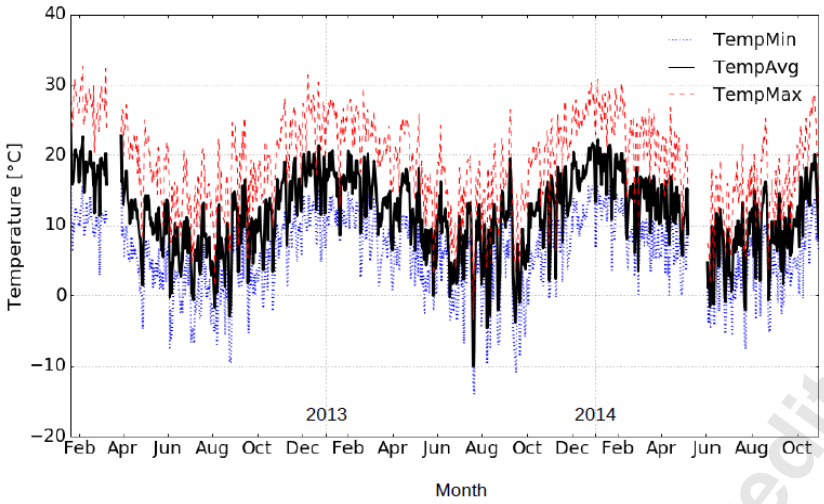

Figure 11. Temporal series of (maximum, mean and minimum) ambient temperature at LEO site. The data were obtained during the day, between 6:00 and 20:00 hours, local time (= UT – 3 hours) in the February 2013 - October 2014 period, employing the Reinhardt MWS 4M weather station.

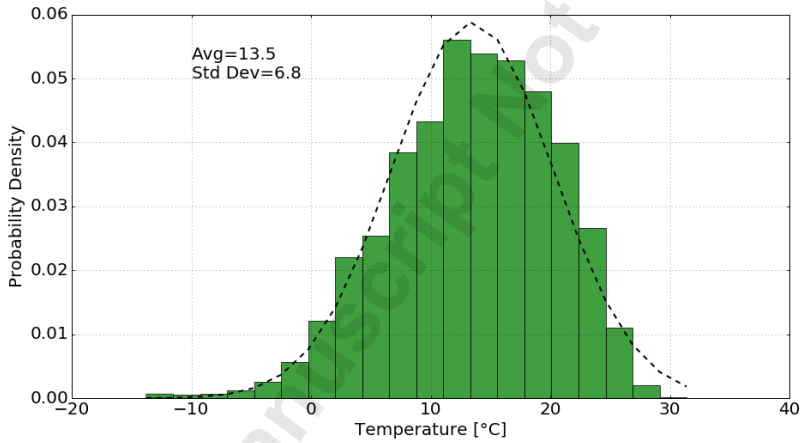

Figure 12. Ambient temperature probability density at LEO site, obtained through a statistical analysis of the data displayed in Figure 11. The broken curve is the corresponding *normal distribution function.*

For the comparison of the air temperature of SAC and LEO sites with respect to Dubai and Ouarzazate sites we used satellite data (see item 2.2.2). The maximum air temperature monthly mean for the four studied sites is shown in Figure 13.Top. For SAC and LEO (Southern hemisphere sites), maximum values in the 16°C –21°C range are recorded during December-January. For the Ouarzazate and Dubai (Northern hemisphere sites) the maximum values are recorded in July-August and are in the 35°C–46°C range, much higher than those observed in SAC and LEO. With respect to the maximum air temperature annual mean, the highest value was obtained for Dubai (35.3°C), followed by Ouarzazate (23.9°C), LEO (14.9ºC) and SAC (13.5ºC) (Figure 13.Bottom). The relative low temperatures of the high altitude with respect to the desert sites have a positive effect if solar photovoltaic power plants are build based in (common) crystalline Silicon panels (see item 3.2).

Journal of Solar Energy Engineering. Received August 06, 2018;
Accepted manuscript posted December 10, 2018. doi:10.1115/1.4042203

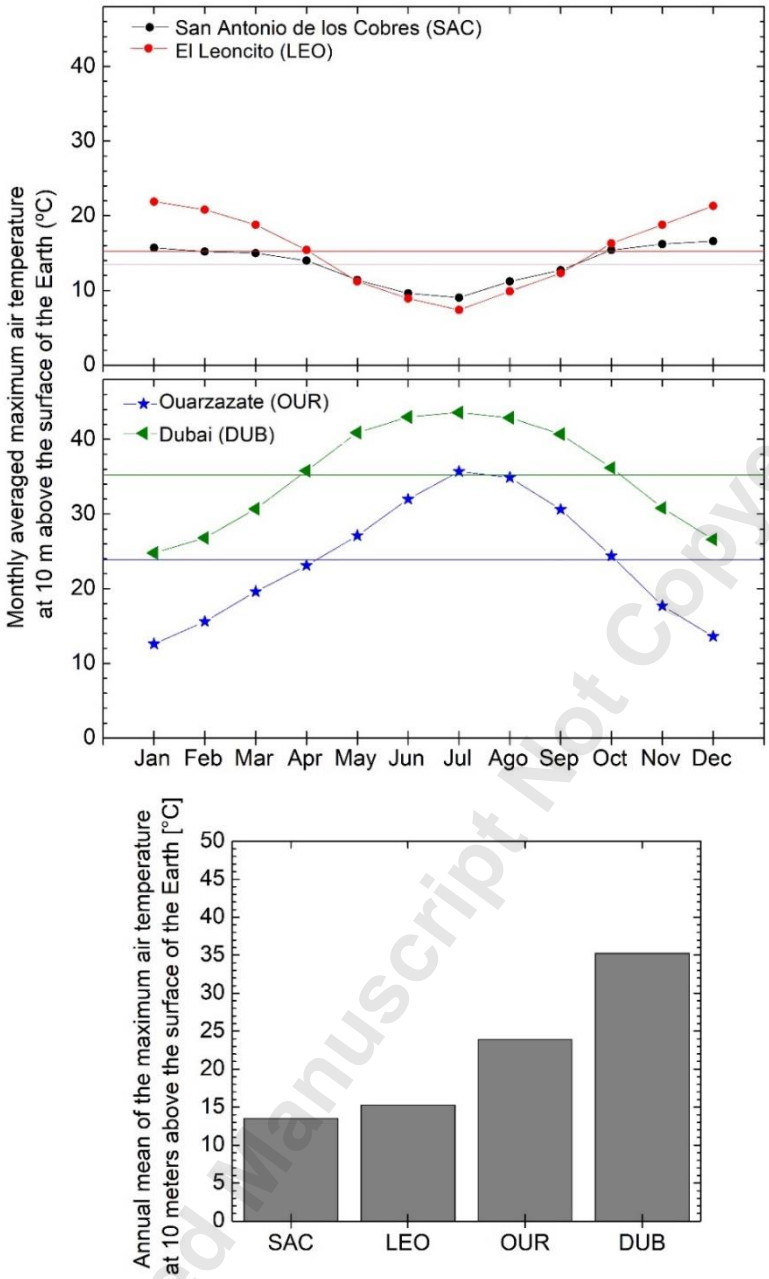

Figure 13.Top. Monthly mean of the maximum air temperature at 10 meters above the ground surface, represented in a similar way as in Figure 5.Top. Source of data: SSE/NASA. Bottom: The same as in Figure 5.Bottom, for the annual mean of maximum air temperature.

We present a similar analysis in Figure 14.Top for the monthly average of the *medium* air temperature. The corresponding annual means (Figure 14.Bottom) are in increasing order: *6.78ºC* (SAC), *9.13 ºC* (LEO), *18.2°C* (Ouarzazate) and *28.5 °C* (Dubai). Concerning the monthly average *minimum* air temperature for these four sites, we display the satellite results in Figure 15.Top. The corresponding annual means (Figure 15.Bottom) are: *1.44 ºC* (SAC), *4.0 ºC* (LEO), *12.4 °C* (Ouarzazate) and *22.1°C* (Dubai).

Journal of Solar Energy Engineering. Received August 06, 2018;
Accepted manuscript posted December 10, 2018. doi:10.1115/1.4042203

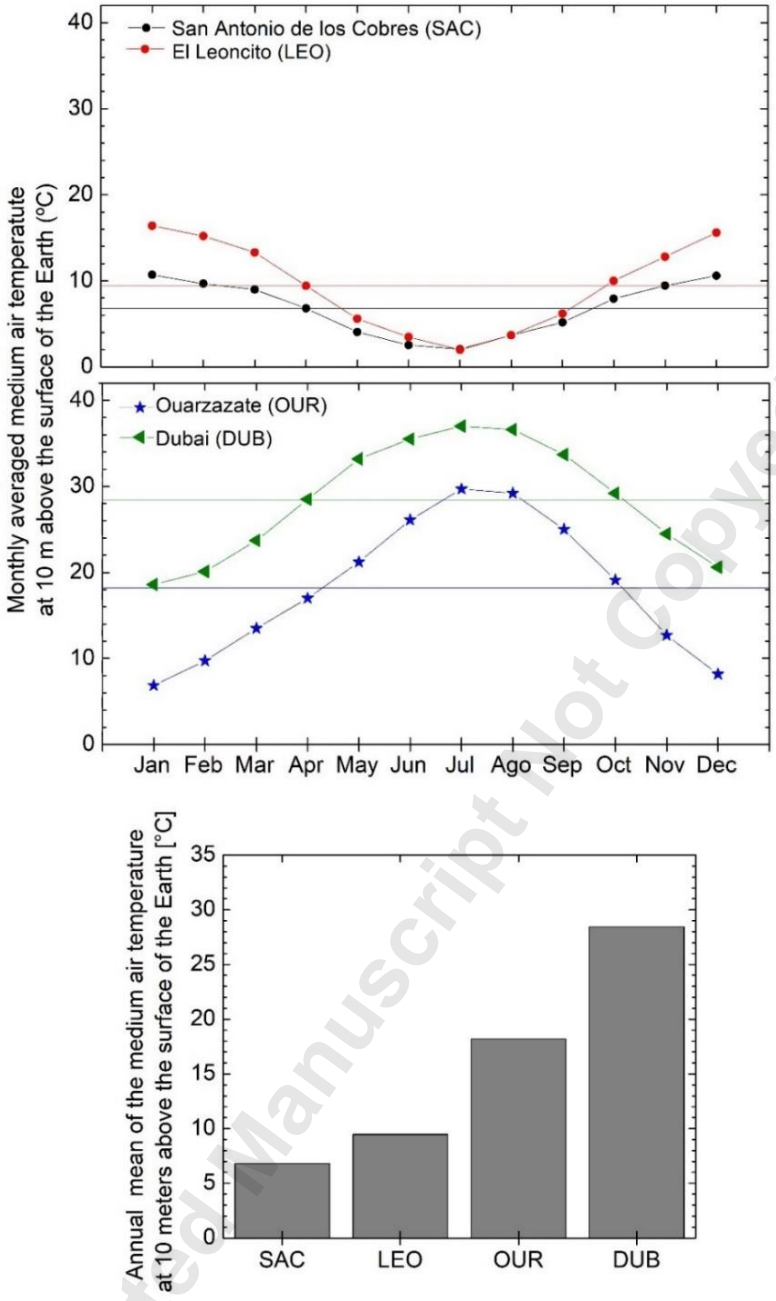

Figure 14.Top. Monthly mean of the medium air temperature at 10 meters above the ground surface, represented in a similar way as in Figure 5.Top. Source of data: SSE/NASA. Bottom: The same as in Figure 5.Bottom, for the annual mean of medium air temperature.

Journal of Solar Energy Engineering. Received August 06, 2018;
Accepted manuscript posted December 10, 2018. doi:10.1115/1.4042203

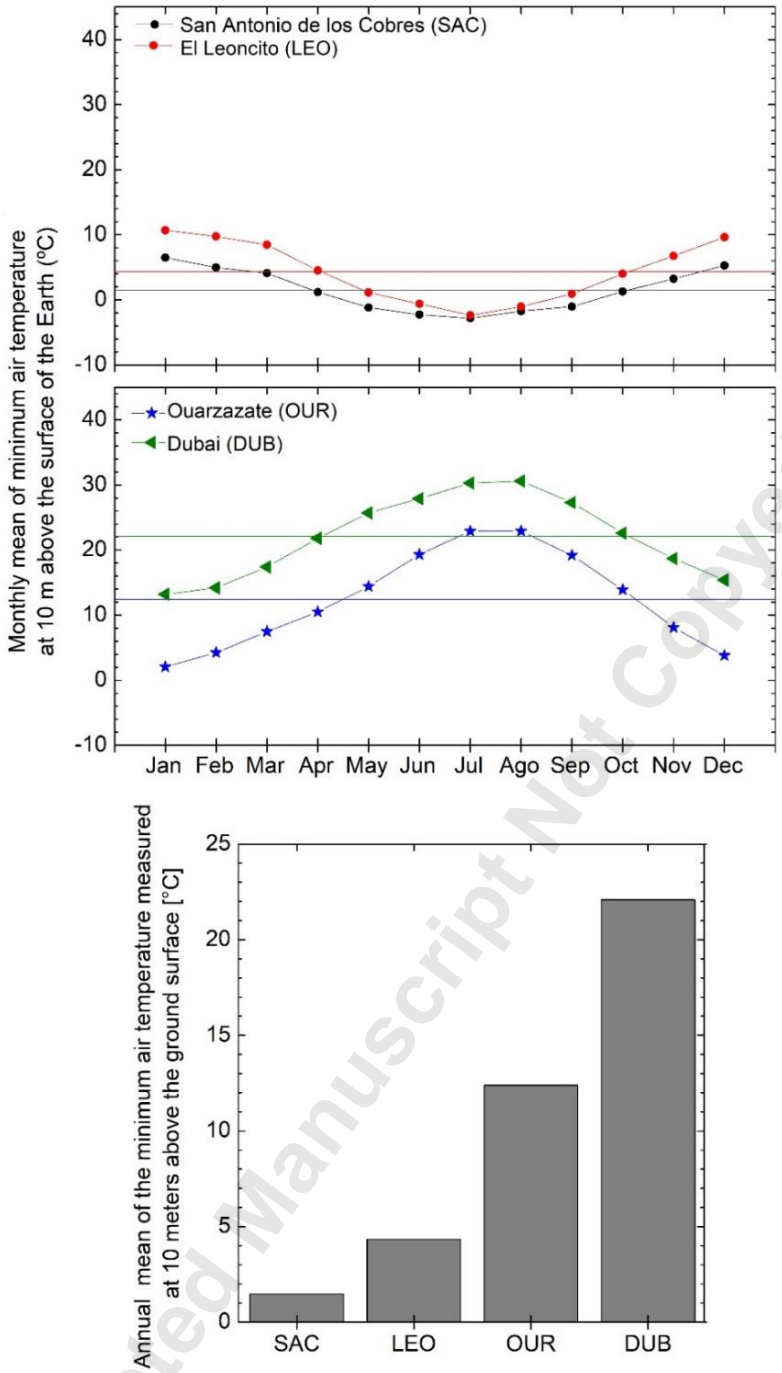

Figure 15.Top: Monthly mean of the minimum air temperature measured at 10 meters above the ground surface, represented in a similar way as in Figure 5.Top. Source of data: SSE/NASA. Bottom: The same as in Figure 5.Bottom, for the annual mean of minimum air temperature.

3.1.5 Relative humidity

Results of relative humidity monthly mean measured at the SAC and LEO sites, are displayed in Figure 16. Annual mean values are 24%for SAC and 25% for LEO. It must be noted that these values change if we consider the daylight time period, showing a decrease in the mean humidity (to 20.3% in SAC and 21.9%

Journal of Solar Energy Engineering. Received August 06, 2018;
Accepted manuscript posted December 10, 2018. doi:10.1115/1.4042203

in LEO). These values, combined with temperature and pressure, can determine some water condensation during hard winter time.

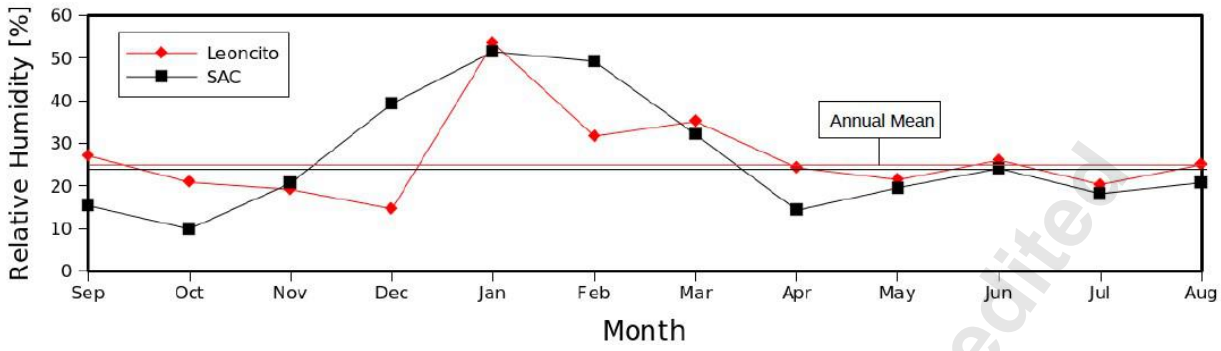

Figure 16. Percentage monthly mean relative humidity in SAC and LEO, obtained with the Reinhardt weather station. The horizontal lines correspond to the annual mean values of SAC (black line) and LEO (red line).

In Figures 17 y 18 we present results of the relative humidity frequency of measured values with the Reinhardt weather station at ground SAC and LEO sites, respectively, in the daylight period. The statistical analysis made in the other previous cases of temperature and relative humidity using a normal (Gaussian) distribution function was not carried out in this case due to the large asymmetry of the frequency data. A way to represent the distribution of relative humidity values around the mean is to determine the 75% percentiles: 29.4% for SAC and 30.8% for LEO.

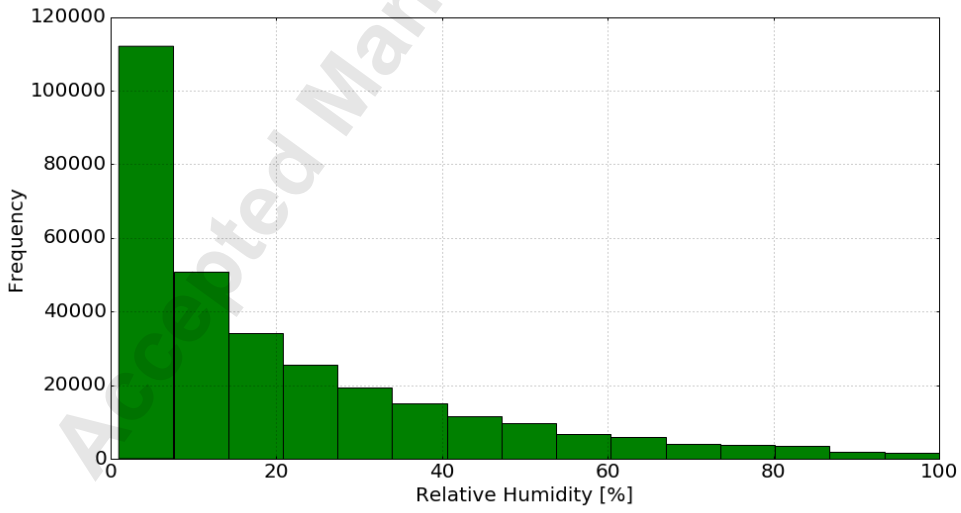

Figure 17. Relative humidity frequency of measured values at mou SAC site, obtained through a statistical analysis of the data registered by the Reinhardt weather station and in the daylight period.

Journal of Solar Energy Engineering. Received August 06, 2018;
Accepted manuscript posted December 10, 2018. doi:10.1115/1.4042203

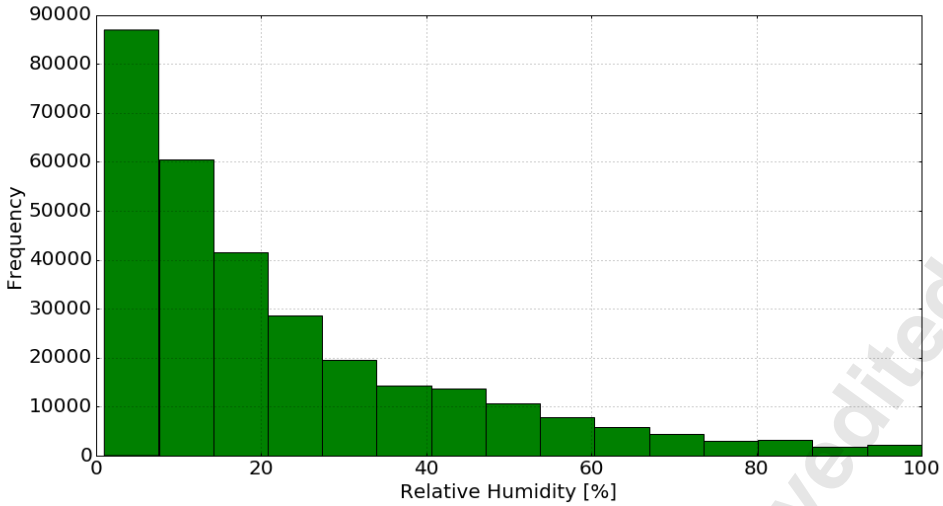

Figure 18. Relative humidity frequency of measured values at ground LEO site, obtained in the same way as for the SAC site (Figure 17).

As previously done for the temperature, satellite data were used for the comparison of the relative humidity of SAC and LEO with Dubai and Ouarzazate sites. Figure 19.Top displays the monthly mean relative humidity for the four sites obtained from the Surface Meteorology and Solar Energy (SSE)/NASA database (see item 2.2.2). SAC presents values quite significant in the Southern hemisphere summer time (DJF), in the *40% - 50%* range (which correlates with the largest precipitations in the year, see for example: https://es.climate-data.org/location/144682/), but the rest of the year is rather low.

The annual mean relative humidity values for each site are the followings*: 38.5%* (SAC), *43.1%* (LEO), *34.9%* (Ouarzazate) and *35.4%* (Dubai) (Figure 19.Bottom). The mean values corresponding to the Argentinean sites are higher than the others two (Ouarzazate and Dubai). Since the derivation of the relative humidity at surface level is particularly difficult from satellite data, this can explain the difference of satellite data from those of the two ground data obtained at the Argentinean places (SAC and LEO). The ground data concentrate mainly in the very low relative humidity range in both sites, as can be seen in Figure 16.

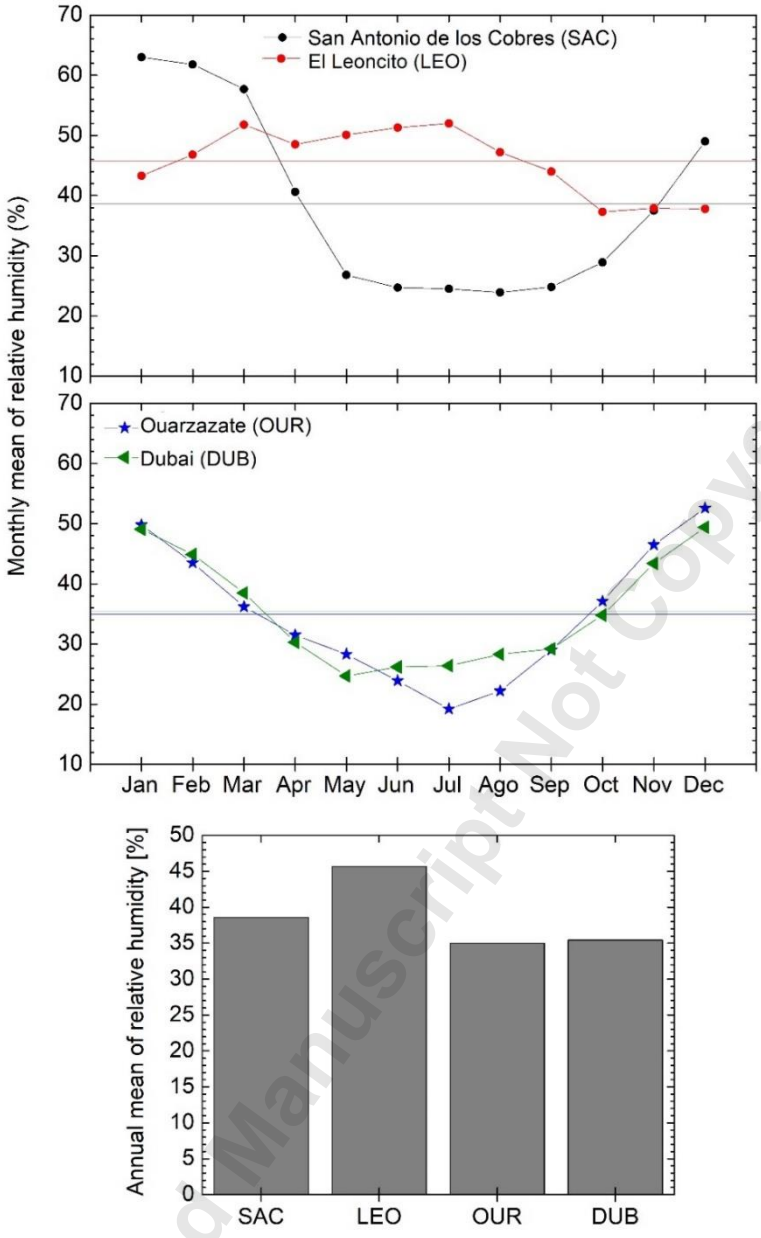

Figure 19.Top. Percentage monthly mean of relative humidity in the four investigated places, represented in a similar way as in Figure 5.Top. Source of data: SSE/NASA. Bottom: The same as in Figure 5.Bottom, for the annual mean of relative humidity.

3.1.6 Wind speed

We determined the wind probably density from wind ground-based measurements at SAC and LEO. The results are presented in Figures 20 and 21. The average in SAC is 14.*8 Km/h (4.11 m/s)* with a standard deviation of *10.5 Km/h* (*2.9 m/s)* and in LEO is *13.5 Km/h (3.75 m/s)* with a standard deviation of *10.0 Km/h* (*2.8m/s)*.

Journal of Solar Energy Engineering. Received August 06, 2018;
Accepted manuscript posted December 10, 2018. doi:10.1115/1.4042203

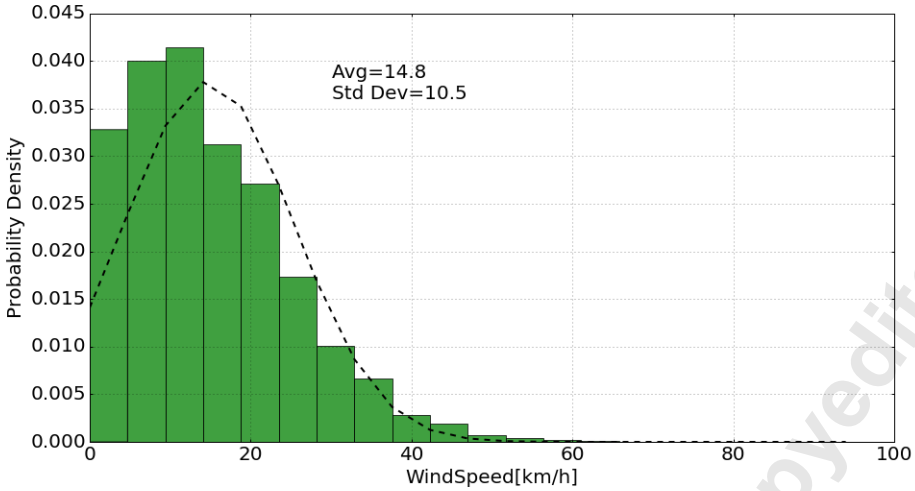

Figure 20. Winds peed probability density at SAC site, obtained through a statistical analysis of the data registered by the Reinhardt weather station. The broken curve is the corresponding *normal distribution function.*

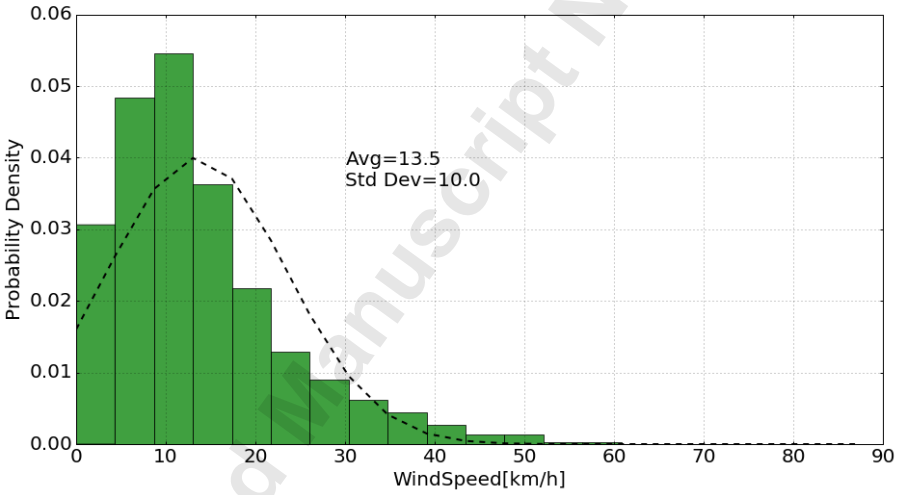

Figure 21. Wind speed probability density at LEO site, obtained in the same way as for the SAC site (Figure 20).

For comparison of the wind speed conditions of SAC and LEO sites with the ones at Dubai and Ouarzazate sites we considered, as in the other cases, the Surface Meteorology and Solar Energy (SSE)/NASA database. The monthly mean of wind speed in the four investigated places are given in Figure 22.Top. The variation is not very significant along the months of the year, since in the case of the Argentinean sites the corresponding minimum-maximum range is 3.3 m/s – 5.2 m/s and for the African and Asian sites, the minimum-maximum range is 3.2 m/s – 4.4 m/s. The annual mean of wind speed for the investigated sites are: 4.35 m/s for SAC, 4.06 m/s for LEO, 3.86 m/s for Ouarzazate and 3.8 m/s for Dubai (Figure 22.Bottom).

Journal of Solar Energy Engineering. Received August 06, 2018;
Accepted manuscript posted December 10, 2018. doi:10.1115/1.4042203

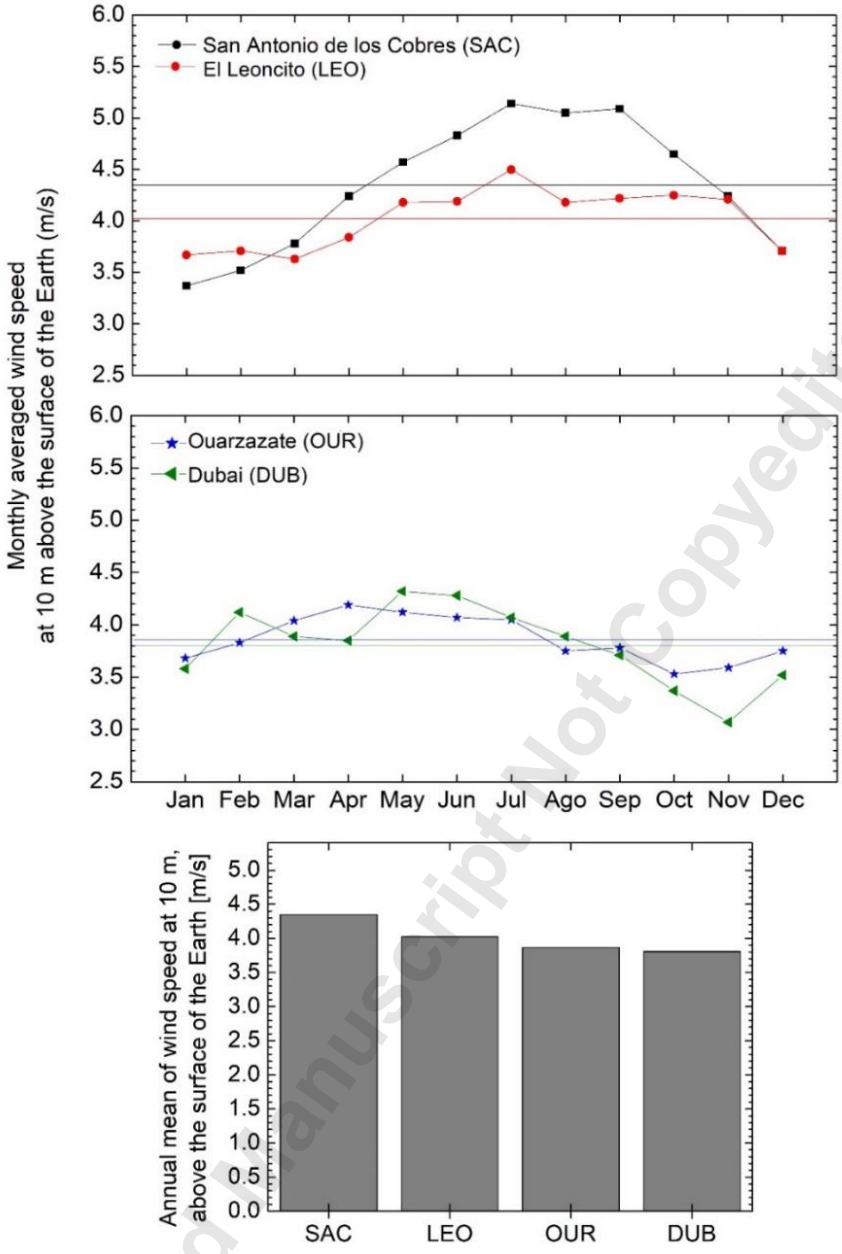

Figure 22.Top: Monthly mean of wind speed in the four investigated places, represented in a similar way as in Figure 5.Top. Source of data: SSE/NASA.Bottom: The same as in Figure 5.Bottom, for the annual mean of wind speed.

3.1.7 Summary statistics of the ground-based meteorological data

In Table 2, we summarized the mean of the normal distribution function and standard deviation (σ) of the significant ground-based meteorological data: temperature, wind speed and the mean and 75% percentile for relative humidity. It must be pointed out that the standard deviation (and 75% percentile) of these variables actually shows the variability range along the months of the year. For example, the temperature at the LEO site, varies from extreme mean values of around *-10 °C* in winter to *30 °C* in summer, as given in Figure 14, explaining the rather large value of the corresponding standard deviation. We also included in

Table 5 the mean results of the *24 hours* data, in order to have a more complete vision of the weather behavior in these sites.

Table 2. Summary of the mean and standard deviation (or 75 % in the relative humidity case) of the ground based meteorological data: T (temperature), RH (relative humidity) and WS (wind speed).

Site	**Daily hours (6:00 to 20:00 hs)**			**Whole day (24 hs)**		
	T ± σ [ºC]	**RH ± 75% percentile [%]**	**WS ± σ [Km/h]**	**T ± σ [ºC]**	**RH ± 75% percentile [%]**	**WS ± σ [Km/h]**
LEO	*13.5 ± 6.8*	*21.9 ± 30.8*	*13.5 ± 10.0*	*11.7 ± 6.6*	*25.6 ± 38.4*	*12.3 ± 8.8*
SAC	*13..0 ± 6.9*	*20.3 ± 29.4*	*14.8 ± 10.5*	*10.5 ± 6.8*	*25.3 ± 37.4*	*13.3 ± 9.6*

The daily hours versus whole day differences in SAC and LEO sites, in the case of ambient temperature, are: ΔT_{LEO} = 1.8 °C and ΔT_{SAC} = *2.5 °C*, higher the daylight time with respect to the whole day, as expected. For the relative humidity, the differences can be detailed in points or percentages: ΔRH_{LEO} = *-3.7 points* (or δRH_{LEO} = *-14.5%*) and ΔRH_{SAC} = -5 points (or δRH_{SAC} = -19.8 %), being negative due to the fact that normally the humidity varies in an inverse relation with respect to ambient temperature. For the wind speed, the differences are, respectively: ΔWS_{LEO} = *9.8 %* and ΔWS_{SAC} = *11.3 %*.

3.1.8 Precipitable water

The monthly mean behavior of precipitable water, obtained from the Surface Meteorology and Solar Energy (SSE)/NASA database (see item 2.2.2), is illustrated in Figure 23.Top. In the case of the Argentinean SAC and LEO sites, a significant variation along the different months of the years is evident, with a maximum in January for these Argentinean sites (*1.1 cm* for SAC and *1.11 cm* for LEO) and a minimum at July (*0.25 cm* for SAC and *0.45 cm* for LEO). The annual mean precipitable water have values as given in Figure 23.Bottom: *0.53 cm* for SAC, *0.73 cm* for LEO, *1.16 cm* for Ouarzazate and *1.95 cm* for Dubai.

Journal of Solar Energy Engineering. Received August 06, 2018;
Accepted manuscript posted December 10, 2018. doi:10.1115/1.4042203

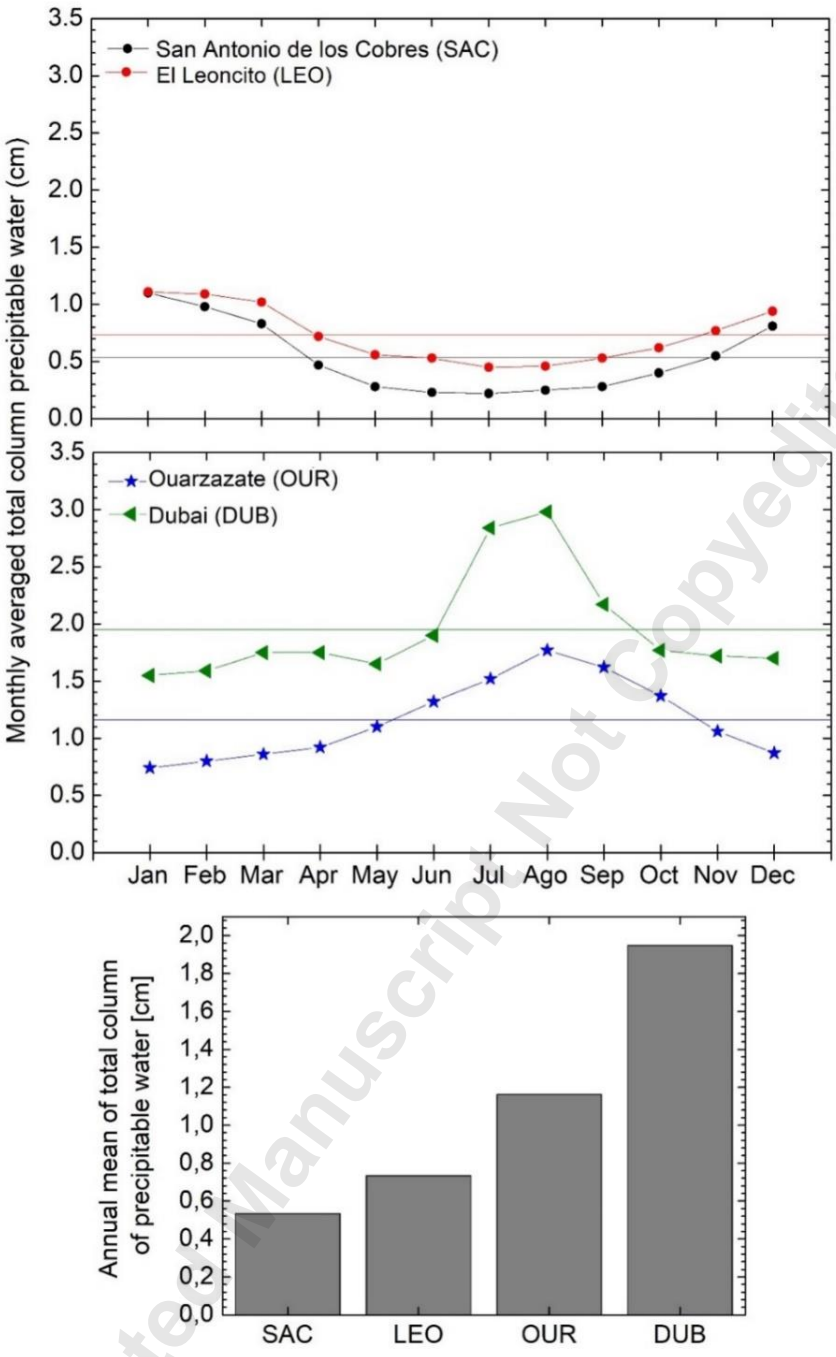

Figure 23.Top. Monthly mean precipitable water (PW) content of the atmosphere at the four sites. Bottom: Annual mean represented in a similar way as in Figure 5.Top. Source of data: SSE/NASA. Bottom: The same as in Figure 5.Bottom, for the annual mean of precipitable water.

3.1.9 Atmospheric aerosols

Atmospheric aerosols have an impact on the PV efficiency in different ways. The most important effect of airborne particles is the attenuation of light due to scattering and absorption. The higher the content of airborne particles (a more turbid atmosphere), the greater the attenuation of the radiation arriving the PV. This phenomenon has a direct negative impact on the efficiency of energy production. This effect is only

Journal of Solar Energy Engineering. Received August 06, 2018;
Accepted manuscript posted December 10, 2018. doi:10.1115/1.4042203

important during the daylight hours. On the other hand, deposited particles on the PV surface produce a screening effect on the radiation arriving the solar device, reducing the effective area of solar energy collection. Depending on the type of aerosols (ocean type, continental dust, biomass or hydrocarbons burning products, etc.) deposited on solar panels, an erosive effect over materials could also be important. Considering particle deposition, it is important to monitor continuously atmospheric aerosol content (not only during daylight), but when considering the scattering/absorption attenuation, it is important to study aerosol content during the sunlight period.

Since high concentration of atmospheric aerosols negatively affects the energy production by reducing the arrival of solar photons on the solar cells to generate electricity, to analyze aerosol content at SAC and LEO sites, the hourly mean mass concentration obtained from the data measured with the GRIMM 1109 aerosol spectrometer (see item 2.2.4) are presented in Figure 24. The straight black line represents the hourly–mean total concentration ($PM_{>0.22}$) while the filled area (in gray color) represents ± 1 standard deviation around the mean. Mass concentration measurements took place during several days on each site (initial and final hour are local UTC -3h, for Argentina): for LEO site from 27th December 2012 (4:10 pm) to 4th January 2013 (5:35 pm) and for SAC from 6th May 2013 (3:32 pm) to 9th May 2013 (3:31 pm).

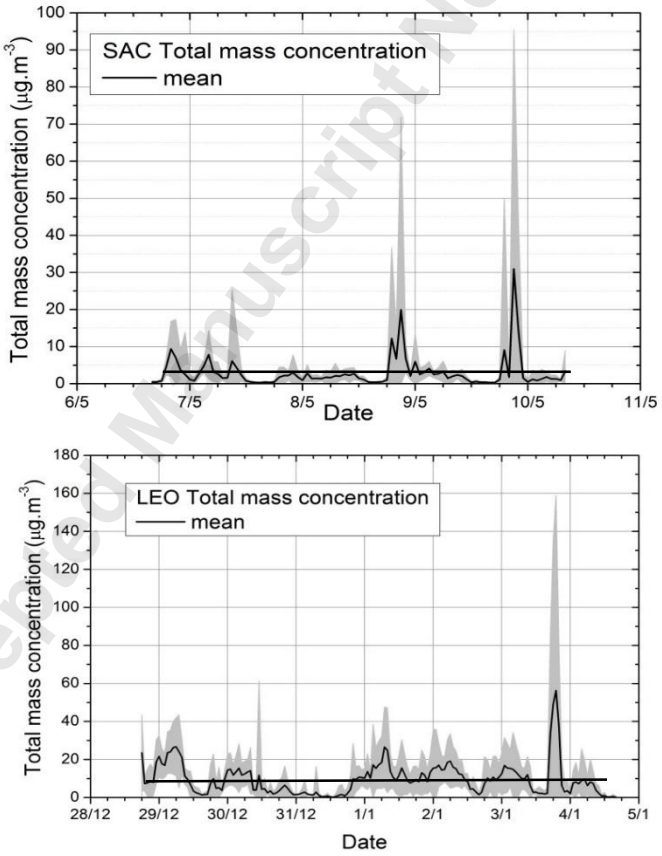

Figure 24. Hourly mean of total mass concentration for the SAC site (top) and for the LEO site (bottom), measured with the GRIMM 1109 aerosol spectrometer.

The reason to take mean values per hour, is to avoid minute-to-minute fluctuations (which can be considerable) on one side, while keeping at the same time, long-term variations in aerosol concentrations. Fluctuations between measurements within the hour are considered by taking the standard deviation as a measure of this dispersion. The mean of the aerosol concentration during the campaign period was 3.0 $\mu g.m^{-3}$ at SAC and 9.6 $\mu g.m^{-3}$ at LEO sites (as shown by the horizontal lines in Figure 24). As shown in Figure 24 for both Argentinean sites, every day the maximum mass concentration values tend to appear during night time (last hours of a given day, and the first ones of the next), showing minimum mass concentration values in the afternoon. So, the lower content of aerosols occurs during daytime, when PV solar energy is produced.

A previous study [12] showed a defined particle concentration behavior during days and nights: During the night, from the late hours of a given day to the first hours of the next, concentrations tend to show its maximum value, then decreasing in the course of the daytime. This can be explained as follows: in daytime, when surface temperature reaches it maximum value, airborne particles distribute better with altitude because of atmospheric convection; while during nighttime, when temperature decreases, the air and the particles suspended are confined near the surface, increasing aerosol concentration values. This is not the only effect on the concentrations, since the daily maximum/minimum value varies day to day, mainly due to wind contribution from outside sources.

In Figure 25 the mean mass concentration during daytime for SAC (left) and LEO (right) are shown. The error bars show the dispersion (standard deviation) around the calculated mean value. The sunlight period mean value for each day was calculated using direct mass concentration measurements. As shown in the mentioned figure these daily mean values appear to be very low.

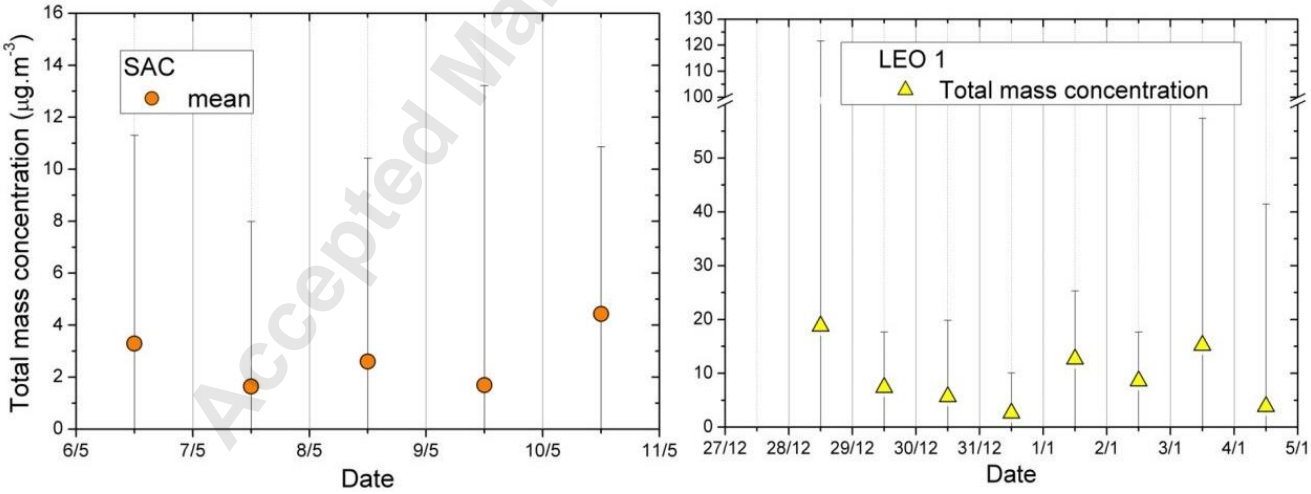

Figure 25. Aerosol mass concentration daily mean during daytime for SAC (left) and LEO (right) sites. Daytime period for each site (local hour UTC -3 h): 8:00 am -9:00 pm for SAC, 7:00 am - 10:30 pm for LEO. Measurements in LEO site from 27th December 2012 (4:10 pm) to 4th January 2013 (5:35 pm) and for SAC from 6th May 2013 (3:32 pm) to 9th May 2013 (3:31 pm).

For comparison of the atmospheric aerosols at SAC and LEO sites with Dubai and Ouarzazate sites, we considered the Aerosol Optical Depth (AOD) measured by the SeaWiFS instrument (on board SeaStar satellite/NASA) at *550 nm* (see item 2.2.5). It must be pointed out that, unlike ground-based measurements, this parameter considers the aerosol content of the entire atmospheric column.

At LEO site, mean AOD is *0.027 ± 0.013* for the 2001-2010 period, with monthly mean values in the range *0.018-0.094* (Figure 26.Top). Moreover, near LEO site, AOD ground-based measurements were also carried out by a Cimel sun photometer at the CASLEO station (*69.30 ºW 31.79 ºS*) of the AERONET/NASA network (https://aeronet.gsfc.nasa.gov see item 2.2.5) in the 2011-2013 period. The mean AOD, measured at a wavelength of *500 nm*, for the 2011-2013 period at CASLEO AERONET station (AOD_{CASLEO}) is *0.027*. In order to compare mean $AOD_{sw,LEO}$ and AOD_{CASLEO}, measured at different wavelengths, we interpolate AOD_{CASLEO} to a wavelength of *550nm* [using the well known Angstrom formula $AOD(\lambda) = \beta/\lambda^{\alpha}$ and considering an Angstrom coefficient $\alpha=1$] and obtained a value of $AOD_{CASLEO}(550) = 0.029$. This value differs only by *6.9%*with respect to $AOD_{sw,LEO}$ (Figure 25.Top). The difference between these values may be due to (at least partially) the fact that they correspond to different periods.

The present results on aerosol at LEO site, from satellite and ground data, show that a PV power plant placed there will have a very low impact on electricity reduction due to dust deposition on the solar panels, since there are very few events of high AOD or aerosol concentration. So, the soiling effect (production of aerosol due to the degradation of soil) is also very small. Another possibility to reduce solar radiation incident on the panels of the PV plant could be snow, but in this site there are no more than three or four not significant snowfalls per year (as confirmed by the personnel of the El Leoncito Astronomical Complex).

At the SAC site, the mean AOD measured by the SeaWiFS instrument ($AOD_{sw,SAC}$) is *0.028 ± 0.013* for the 2001-2010 period, with mean monthly values in the range 0.*018-0.10* (Figure 26.Bottom).

The mean AOD at Ouarzazate and Dubai was also analyzed. The mean AOD measured by the SeaWiFS instrument ($AOD_{SW,OUARZAZATE}$) is *0.25 ± 0.13* for the 2001-2010 period, with monthly AOD mean values as high as *0.74* and minimum of *0.09* (Figure 26.Top). At Dubai the mean AOD measured by the same satellite instrument and in the same period ($AOD_{SW,\ DUBAI}$) is *0.39 ± 0.11*, with monthly AOD mean values in the *0.16-0.60* range.

Journal of Solar Energy Engineering. Received August 06, 2018;
Accepted manuscript posted December 10, 2018. doi:10.1115/1.4042203

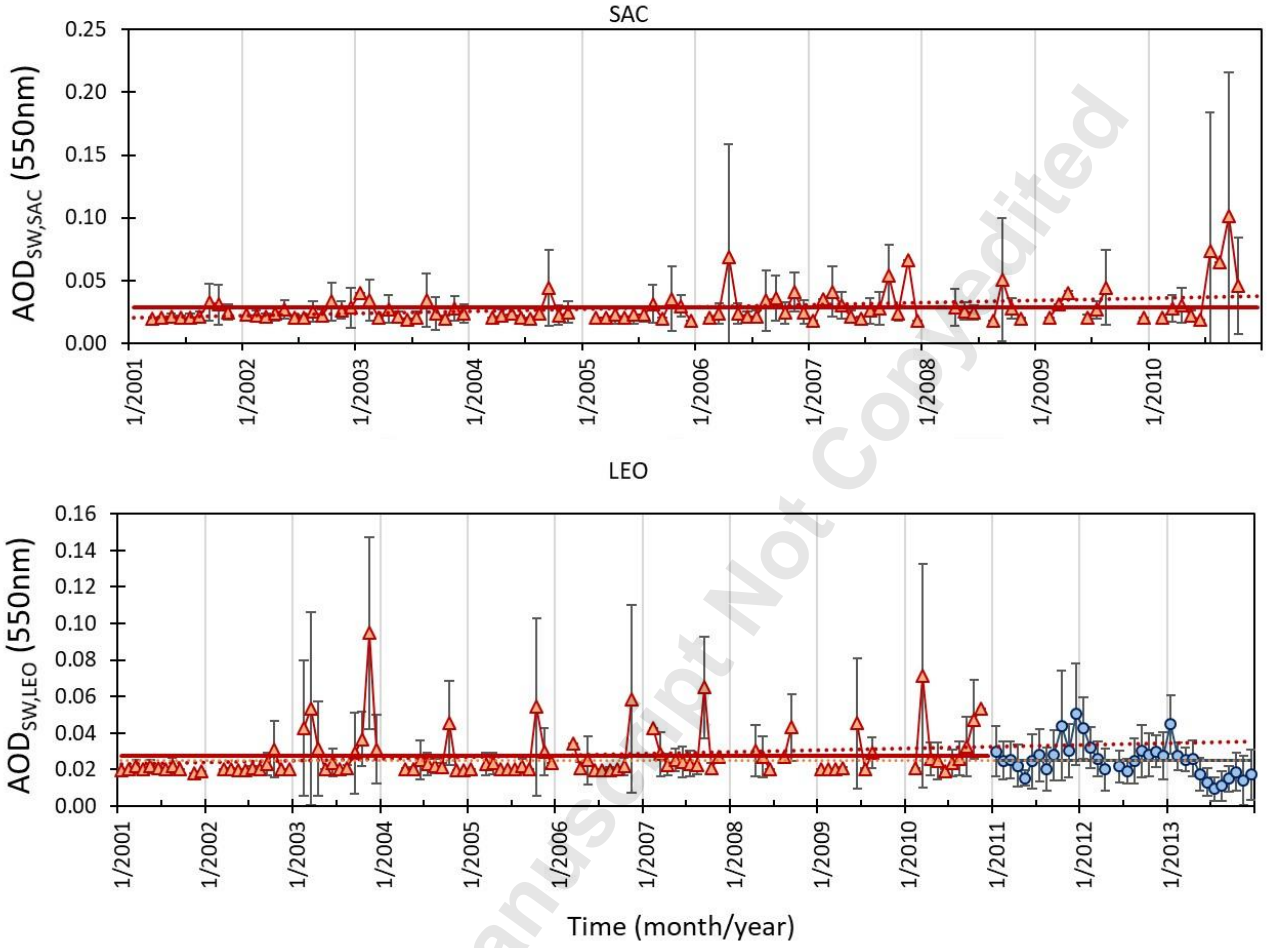

Figure 26. Aerosol Optical Depth at *550 nm* measured by the SeaWiFS sensor (SeaStar satellite/NASA) for the two Argentinean sites: SAC (top) and LEO (bottom) (orange triangle and segment, monthly mean and standard deviation, respectively) and measured by CASLEO AERONET station (blue square and segment; see section 2.2.5). Note: the horizontal line is the mean value of *0.028* for SAC and *0.027* for LEO and the dotted line corresponds to the lineal trend: *0.0018 per year* for SAC and 0.0010 p*er year* for LEO.

The mean AOD values at Ouarzazate and Dubai, are at least 750% higher than the mean values measured for SAC and LEO sites. Moreover, we analyzed how it is expected to continue the time evolution of aerosol content of the atmosphere at both Argentinean sites (SAC and LEO). Assuming no significant changes with respect to the past evolution of aerosols and considering the observed trend at each site (represented in Figure 25 by the dotted lines), we determined that by December 2047 (at the estimated end of life of the solar power plants), the average of AOD for SAC and LEO sites will be approximately of *0.104* and *0.070*, respectively. These estimated values are still well below the mean AOD observed at Ouarzazate and Dubai sites, which do not show a definitive trend (see Figure 27).

Journal of Solar Energy Engineering. Received August 06, 2018;
Accepted manuscript posted December 10, 2018. doi:10.1115/1.4042203

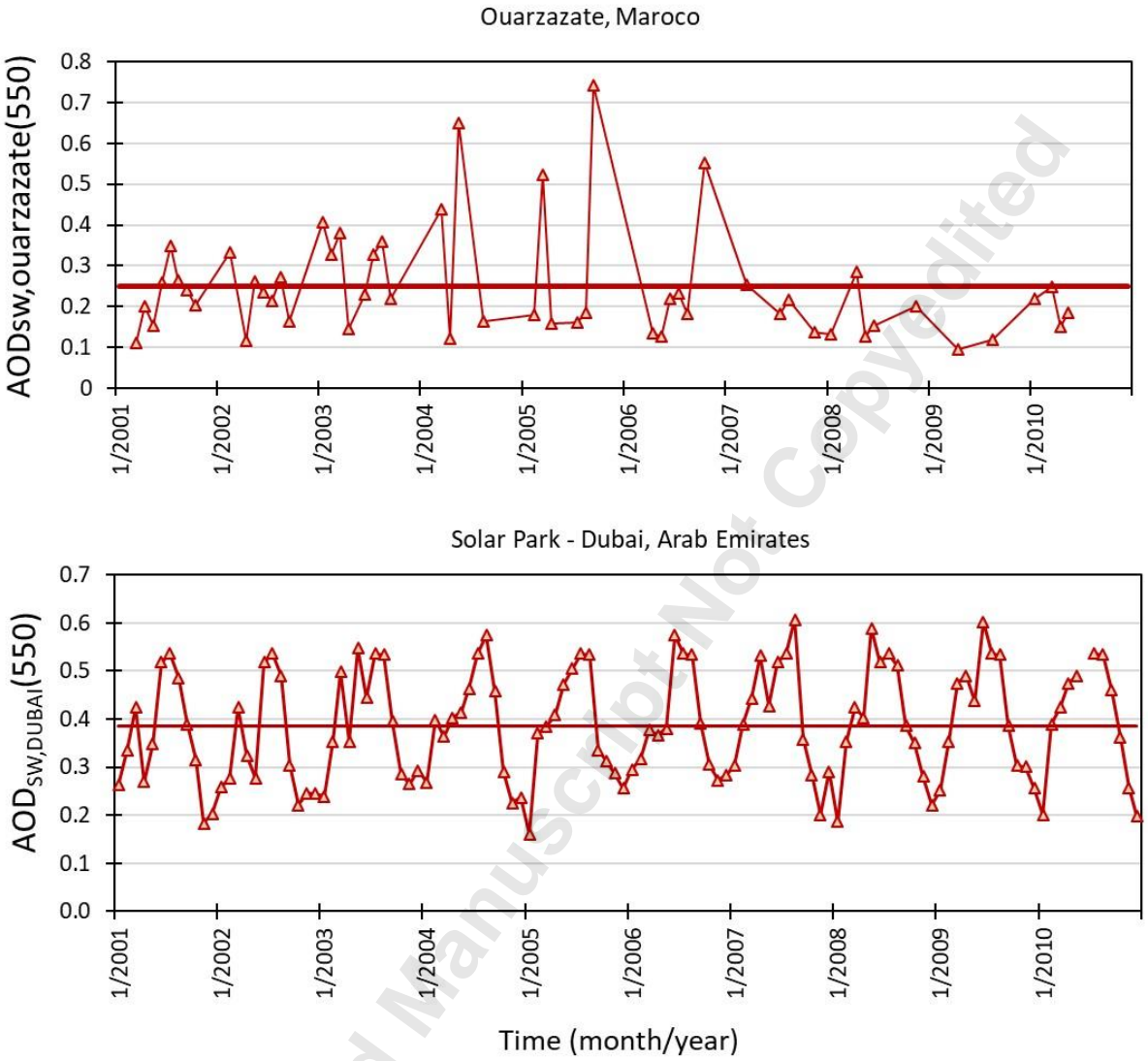

Figure 27. Aerosol Optical Depth at *550nm* measured by SeaWiFS sensor (SeaStar satellite/NASA) for the African and Asian sites, respectively: Ouarzazate (top) and Dubai (bottom) (orange triangle and segment). Note: the horizontal line is the mean value of *0.25* for Ouarzazate and *0.39* for Dubai.

Concerning the atmospheric aerosols, the SAC and LEO sites, with AOD values being at least one order of magnitude lower than those of Ouarzazate and Dubai, have better conditions than these other two sites where large solar power plants have been (or will be) built.

We like to point out that the Andes volcanic eruptions could be a source of aerosol emissions and consequently a problem for the considered sites, but, even if the Andes region is situated in the so called Pacific ring of fire, in a previous work, Della Ceca et al [30] demonstrated that the most significant eruption produced in April 19 and 20, 1993 by the Lascar volcano, placed rather near SAC (162 Km to the NW), only affected a few days this region. A similar situation happened with LEO site, with the more recent

eruption, in June 2011, of the Puyehue/Cordón Caulle volcanic complex at Chile Patagonia. Except these two events very concentrated in time, no other volcanic eruptions (that needs to be combined with winds in the SAC and LEO directions), introduced particulate matter in the atmosphere in a significant proportion.

3.2 Energy generation estimation

The importance for the placement of solar power plants in San Juan Province (Argentina) was highlighted by Margulis [30] that analyzed the consumption of electricity in this province during February (summertime in the Southern Hemisphere) where a broad (maximum) peak of 480 MWh was registered at about the center of the period between 2:00 to 6:00 pm, mainly due to the use of air conditionings. It coincides with a significant portion of the time period were a solar power plant could produce energy. So, the author concluded, extrapolating the energy production of the (small) solar power plant Cañada Honda 2 (3 MWp) to a larger one that could cover the demand at the peak indicated above (480 MWh), that an energy saving of about 7.5% could be obtained, due to reduction in electric losses produced by transportation and distribution form the National Electric Interconnected System (NEIS).

Considering the PV power calculator developed by the World Bank Group (http://globalsolaratlas.info), we calculated the *potential photovoltaic electricity production factor (PV_{out})* for the four sites considered in this study. Results are shown in Table 3 together with the solar radiation incident on the optimum (near latitude) inclined angle, the annual solar irradiation (on horizontal and inclined surfaces) and the percentage relative differences of this factor with respect to SAC (which has the largest factor).

Table 3. Optimal elevation angle, annual mean ambient temperature, annual mean global solar (horizontal and tilted) irradiation, percentage difference of tilted vs horizontal irradiation, potential photovoltaic electricity production factor and percentage difference corresponding to this factor, for two Argentina East Andes range sites: San Antonio de los Cobres (SAC) and El Leoncito (LEO), one African site (Ouarzazate, Morocco - OUR) and one Asian (Dubai, United Arab Emirates - DUB) site.

Site	Optimal elevation angle	Annual mean temperature (°C)	Annual global solar horizontal irradiation [KWh/(m^{2}year)]	Annual global solar tilted (to the optimum angle) irradiation [KWh/(m^{2}year)]	Percentage difference of tilted vs horizontal irradiation	Potential photovoltaic electricity production factor, PV_{out} [kWh/(kWpyear)]	Percentage difference in PV_{out}, with respect to SAC
SAC	26°	6.78	2263	2394	5.80%	2304	-----
LEO	31°	9.13	2055	2212	7.60%	2143	-7.00%
OUR	31°	18.2	1971	2139	8.50%	1 940	-15.80%
DUB	25°	28.5	2055	2124	3.40%	1 780	-22.70%

From the annual mean of the medium air temperatures for the four sites given in Table 3 and assuming the dependence of the quantum efficiency with temperature given before (*0.4% per °C*), a given solar panel subject to these temperatures will have at SAC, *0.94%* more efficiency than at LEO, *4.6%* more than at Ouarzazate and *8.7%* more than at Dubai.

In the next sections we estimate the PV power that a solar park could produce at SAC and LEO sites.

3.2.1 SAC site and adjacent region

The possible area to be employed for the placement of solar power plants at the SAC region is derived from Figure 2.Top and area the extension described in item2.1.1, as follows: A_{sac} = *16.6 x 5.4* Km^2= *8960 hectares*. It must be pointed out that a similar analysis can be made for concentrated solar power (CSP) plants. Since it is needed about *1.5 hectares* for each *1* MW_{peak} of solar PV power and assuming that *10%* of the whole terrain surface is used for other applications: routes, buildings for inverters and persons, transmission lines, town expansion, etc.(actually there is more place around the borders), the total SAC installed PV power of the whole plant will be:

$$P_{PV,SAC} = 0.9*A_{SAC}/(1.5\ hectares/MW_{peak}) = 5380\ MW_{peak} \quad (3)$$

To obtain the electric energy produced, we considered as a reference the technical characteristics included in the PV power calculator (PVWatts) developed by the National Renewable Energy Laboratory (NREL) of United States. We assumed the following PV ground-mounted large scale solar system technical characteristics: *Module type*: Si crystalline (premium quality) of 19 % efficiency, *array type*: fixed, *array tilt*: 20º North oriented, *system losses*: 12 % (including: *shading* due to mountains in the far away horizon: 2 %, *mistmatch* due to electrical losses by electrical losses due to small differences caused by manufacturing imperfections between modules: 2 %, *wiring/connections* produced by resistive losses in the DC and AC wires and electrical connections: 2.5 %, solar radiation degradation of PV solar cells in the initial years: 2.5 %, *nameplate rating* accounts for the accuracy of the values given by the manufacturer: 1 % and *availability* due to reduction in the system's output cause by operational factors like scheduled and unscheduled system shutdown for maintenance and grid outages: 2 %), *inverter efficiency*: 96 %, *DC to AC size ratio*: 2%). We like to point out that, from the present results of extremely low aerosol content of the atmosphere in SAC (and also in LEO) Andes range, as was analyzed in item 3.1.9, the *soiling* effect (deposition of particulate matter on the panels reducing the incidence of solar radiation) is assumed to be practically zero.

Employing the PV power calculator developed by the World Bank Group, we obtain a value of the *Potential photovoltaic electricity production factor* also called *Solar PV merit factor* (that measures the efficiency to produce electricity of a given solar PV system placed at a given site): $f_{PV,\ SAC}$ = *2304* kWh/kW_{peak}*per year (see Table 3).* So, the electricity that will produce annually the SAC region would be:

$$E_{PV,SAC} = 0.88*(f_{PV,SAC}* 5380\ MW_{peak}) = 10.9*10^6 MWh\ per\ year \quad (4)$$

where the factor 0.88 came from the proposed (typical) system losses. The difference of this produced energy value with respect to that determined with the PVWatts calculator (assuming it can be extended to the present study) is only: $\Delta E_{PV} = 100*(E^*_{PV,SAC} - E_{PV,SAC})/E_{PV,SAC} = 9.2$ %.

The percentage uncertainty of the produced energy value can be estimated from the individual values of the uncertainty in the installed PV solar power plant of u_P=10 % and in the coefficient $f_{PV,\ SAC}$, of u_f = 5%.

Then, the uncertainty in the electric energy produced annually is: $u_E = [(10\ \%)^2 + (5\%)^2]^{1/2} = 11.2\%$. Consequently, the final result will be:

$$E_{PV,SAC} = (10.9 \pm 1.2)*10^6 MWh\ per\ year \quad (5)$$

Since Argentina has a national electric matrix highly dependant on fossil fuels (as was stated in the Introduction) and considering the conversion coefficient between a unit of mixed electric energy (renewable and non renewable) of the country and a unit of emited greenhouse gases (GHG), $f_{E,GHG}(Arg) = 0.535\ tons\ of\ CO2_{eq}/MWh$ [19], this solar PV clean electricity production will avoid the annualemission of the following mass of GHG:

$$M(GHG)_{PV,SAC} = f_{E,GHG}(Arg)*E_{PV,SAC} = 5.83*10^6 tonsCO2_{eq}\ per\ year \quad (6)$$

where the unit, including the word *equivalent* (or *eq*), means that the emitted GHG are referred all of them (Methane CH4, Nitrous oxide N2O, etc.) to CO2 through the corresponding Global Warming Potentials (100 years time horizon):28 for CH4 and 165 for N2O, as given in the report of IPCC [32]. We like to point out that the situation is dynamic and the coefficient could change along the years, for example, due to the inclusion of renewable energy sources like those proposed in the present work.

3.2.2 LEO site and adjacent region

For this site, we consider the data derived from Figure 3.Top and area extension described in item 2.1.2. We determined the possible area to be used for the placement of solar PV power plants in the LEO region as follows: $A_{LEO} = 178.1\ Km^2 = 17810\ hectares.$

Making the same assumption as in the SAC case for the derivation of formula (3), the total LEO installed PV power of the whole plant will be:

$$P_{PV,LEO} = 0.9*A_{LEO}/(1.5\ hectares/MW_{peak}) = 10690\ MW_{peak} \quad (7)$$

In a similar way as was done for obtaining the Solar PV merit factor in the SAC case, we determined the following value of the LEO Solar PV merit factor: $f_{PV,LEO} = 2143\ kWh/kWp\ per\ year$(Table 3). Consequently, the electricity that will produce annually the LEO region would be:

$$E_{PV,LEO} = f_{PV,LEO}*5380\ MW_{peak} = 11.53*10^6\ MWh\ per\ year \quad (8)$$

Assuming the same percentage reduction of 12 % due to system losses in this energy value and the same percentage uncertainty for the produced energy in SAC site, for LEO site

$$E_{PV,LEO} = (10.1 \pm 1.1)*10^6 MWh\ per\ year \quad (9)$$

The sum of the electrical energy that would be produced annually by the SAC (formula 5) and LEO (formula 9) regions, with its corresponding uncertainty, is:

$$E_{PV,SAC+LEO} = (21.0 \pm 2.3)*10^6\ MWh\ per\ year \quad (10)$$

In a similar way as was determined for the emitted GHG in the case of SAC (formula 6), for the LEO site results:

$$MGHG_{PV,LEO} = f_{E,GHG}(Arg)*E_{PV,LEO} = 5.40*10^6 tons\ of\ CO2_{eq}\ per\ year \quad (11)$$

Consequently, the total contribution of both (SAC and LEO) sites, from formulas (6) and (11), is:

$$MGHG_{PV,SAC+LEO} = 11.2*10^6 tons\ of\ CO2_{eq}\ per\ year \quad (12)$$

In 2015, Argentina employed $134.5*10^6$ *MWh* of electricity [33]. So, considering the possible annual PV electric supply by the SAC and LEO regions given in formula (10), these two sites could provide around *15.6 %* of the total energy, if in the future the electric energy use in Argentina continues to be the same, by the introduction of energy efficiency measures that will *decarbonize*the economy, separating Gross Domestic Product increase from energy intensity decrease.

4 Conclusions

The results obtained in this study evidence that San Antonio de los Cobres (SAC) and El Leoncito (LEO) sites, and their considered adjacent regions, placed in the Argentinean Andes range, are very suitable sites for the placement of solar power plants, due to the sum of very important factors: a) high solar irradiation in a large fraction of days of the year and consequently very high annual mean solar irradiation (6.56 kWh/m^{2}day for SAC and 5.45 kWh/m^{2}day for LEO sites), b) extremely low atmospheric particulate matter (aerosol optical depth 0.028 for SAC and 0.027 for LEO, and 3.0 μg.m^{-3} for SAC and 9.6 μg.m^{-3} for LEO), c) low water content of the atmosphere (0.53 cm for SAC and 0.73 cm for LEO), d) low mean ambient temperature (6.8 °C for SAC and 9.5°C for LEO) and e) high altitude consequently, low air mass (3607 m a.s.l for SAC and 2627 m a.s.l for LEO). Another points to be highlighted is the high solar transmittance of the atmosphere since the proposed sites are of high altitude with almost no perturbation due to natural events, even volcanic eruptions, as indicated in item 3.1.9.

Concerning the selection of the geographical placement of the selected SAC and LEO sites we like to point out that these rather flat areas are quite unique in comparison with the adjacent Andes regions, since in these last regions there are mountain peaks that are within the highest in all the Andes range.

The results presented in this work, mainly for the daytime period in two sites of the Andes range, are of importance for fixing the *sky clearness* at present and consequently to be as a comparison reference for the future evolution of this variable, due to the possible increase in natural air contamination.

These results for typical places of the Argentina Andes, can be extended to near regions with rather similar characteristics. The comparison with sites where solar power plant projects already exist (Ouarzazate, Morocco and Dubai, United Arab Emirates), shows that Argentine sites have even more favorable atmospheric conditions and solar radiation behaviors for the generation of solar energy. We like to point out that the use of data provided by the *same satellite* over passing the four sites in the *same period of years*, gives confidence in the comparison of solar radiation and climatic data.

In the present work, we also obtained results of the possible production of electricity that could be introduced into the Argentina National Interconnected System and produced in both Argentinean regions. They could supply about *21000 GWh per year*, with is *15.6 %* of the 2015 Argentina electric consumption. Consequently, the emission of greenhouse gases can be reduced in a total mass of *11.2 million tons of* $CO2_{eq}$ *per year*. This value can be compared with the net emission of greenhouse gases made by Argentina in 2014 (the year with the last information) of 368 million tons of GHG [33]. The contribution to the reduction in the corresponding emission could be about 3%.

The present results are a significant source of information for those interested in the development of solar (concentrated or distributed)power plants, since normally it is needed at least a year for the *in situ* study of each possible place, before to determine its feasibility.

The placement of solar power plants at the proposed SAC and LEO sites could partially provide electricity not only to all the country through the National Electric Interconnected System,-avoiding frequent cutoff of electric power supply, mainly in summer, but also to isolated (low income) populations leaving in the Argentina Andes range. They could also reduce the large dependence that Argentina has on imported oil and natural gas for the thermoelectric plants, which are largely subsidized.

Acknowledgements

This work has been developed within the PIP CONICET N° 0405 project. We also acknowledge the support of Ministerio de Ciencia, Tecnología e Innovación Productiva de la Nación and CNEA. The authors acknowledge the Science team responsible for the operation and maintenance of the Surface Meteorology and Solar Energy (SSE)/NASA and SeaWiFS/NASA databases and the AERONET network.

References

[1] International Energy Agency (IEA), 2017. Key world energy statistics. IEA Publications, International Energy Agency. France, September 2017 Available at https://www.iea.org/publications/freepublications/publication/KeyWorld2017.pdf

[2] OLADE (Organización Latinoamericana de Energía). "Anuario de estadísticas energéticas". Edited by OLADE, Quito, Ecuador, 2017 (ISBN 978-9978-70-127-0).

[3] IPCC (Interguvernmental Panel on Climate Change), Working Group I. "Climate change 2013: The physical science basis". Cambridge University Press, 2013 (also available at: www.ipcc.ch).

[4] García-Cascales M.S., Lamata M.T. Sánchez-Lozano J.M. "Evaluation of photovoltaic cells in a multi-criteria decision making process". Annals of Operations Research, 199, 373-391, 2012.

[5] Bhubaneswari P., Iniyan S., Ranko G. "A review of solar photovoltaic technologies". Renewable and Sustainable Energy Reviews, 15, 1625-1636, 2011.

[6] Piacentini, R.D., Cede, A. and Bárcena, H. "Extreme solar global and UV irradiances due to cloud effect measured near the summer solstice at the high altitude desertic plateau Puna of Atacama". Journal of Atmospheric and Solar Terrestrial Physics, 65, 727-731, 2003.

[7] https://irena.masdar.ac.ae/gallery/#map/3103

[8] Ebad M and Grady W M. "A cloud shadow model for analysis of solar photovoltaic power variability in high-penetration PV distribution networks". Proceedings Power and Energy Society General Meeting, Published by IEEExplore, November 2016, DOI: 10.1109/PESGM.2016.7742024.

[9] Roy, J. N., Bose, D.N. Photovoltaic Science and Technology. Cambridge University Press, page 281, 2018.

[10] Liu J, Fang W, Zhang X, and Yang. "An improved photovoltaic power forecasting model with the assistance of aerosol index data". IEEE Transactions on Sustainable Energy, 6, (2), 434-442, 2015.

[11]http://www.power-technology.com/projects/miraah-solar-thermal-project/miraah-solar-thermal-project5.html

[12] Gambetta P and Doña P M. "Planta solar fotovoltaica Solar San Juan I: Descripción de su diseño y detalles de su construcción". Proceedings Cuarto Congreso Nacional–Tercer Congreso Iberoamericano Fuentes Sustentables de Energía, HYFUSEN, 11-258, 2011. (Available at: http://www.cab.cnea.gov.ar/ieds/images/2011/hyfusen_2011/trabajos/11-258.pdf).

[13] Belmonte, S., Núñez, V., Viramonte, J.G., Franco, J. "Potential renewable energy resources of the Lerma Valley, Salta, Argentina for its strategic territorial planning". Renewable and Sustainable Energy Reviews, 13, (6), 1475-1484, 2009. https://doi.org/10.1016/j.rser.2008.09.014.

[14] Piacentini, R.D, García, B, Micheletti, M.I, Salum, G, Freire, M, Maya, J, Mancilla, A, Crino, E, Mandat, D, Pech, M, Bulik, T. «Selection of astrophysical/astronomical/solar sites at the Argentina East Andes range taking into account atmospheric components». Advances in Space Research, 57(12)2559-2574, 2016.

[15] http://www.usgbc.org/

[16] Bai, J., Chen, X., Dobermann, A., Yang, H., Cassman, K.G., Zhang, F. Evaluation of NASA satellite- and model-derived weather data for simulation of maize yield potential in China. Agronomy Journal, 102, 9-16, 2010.

[17] White, J., Hoogenboom, G., Stackhouse, P.W., Hoell, J.M. Evaluation of NASA satellite- and assimilation model-derived long-term daily temperature data over the continental US. Agricultural and Forest Meteorology 148, 1574-1584, 2008.

[18] White, J., Hoogenboom, G., Wilkens, P.W., Stackhouse, P.W., Hoell, J.M. Evaluation of Satellite-Based, Modeled-Derived Daily Solar Radiation Data for the Continental United States. Agronomy Journal, 103, 1242-1251, 2011.

[19] Gueymard C A."SMARTS2, a simple model of the atmospheric radiative transfer of sunshine: algorithms and performance assessment", Report FSEC-PF-270-95, University of Central Florida, USA, December 1995.

[20] Gueymard C A. "Clear-sky irradiance predictions for solar resource mapping and large-scale applications: Improved validation methodology and detailed performance analysis of 18 broadband radiative models". Solar Energy, 86 (8) 2145-2169, 2012.

[21]Microprocessor Weather Station MWS 4M Manual. Available at: www.reinhardt-testsystem.de/_pdf/english/mws4m_e.pdf

[22] Mandat D., Miroslav P., Miroslav, H., Schovanek, Prouza M., Travnicek P., Janecek, P., Ebr, J., Doro, M., Gaug, M., for the CTA Consortium. All Sky Camera for the CTA atmospheric calibration work package. EPJ Web of Conferences 89 03007, 2015.

[23] Portable Laser Aerosol spectrometer and Dust Monitor Manual, Model 1.108/1.109. Printed in Germany. Copy Right © 2010 by GRIMM Aerosol Technik, Ainring. Available at http://www.wmo-gaw-wcc-aerosol-physics.org/files/opc-grimm-model--1.108-and-1.109.pdf

[24] https://www.esrl.noaa.gov/gmd/grad/solcalc/sunrise.html

[25] Holben B.N., T.F.Eck, I.Slutsker, D.Tanre, J.P.Buis, A.Setzer, E.Vermote, J.A.Reagan, Y.Kaufman, T.Nakajima, F.Lavenu, I.Jankowiak, and A.Smirnov. AERONET - A federated instrument network and data archive for aerosol characterization, Rem. Sens. Environ., 66, 1-16, 2018.

[26] https://disc.gsfc.nasa.gov/datasets/SWDB_L3MC05_004/summary

[27] https://giovanni.gsfc.nasa.gov/giovanni/

[28] www.power-technology.com/projects/noor-ouarzazate-solar-complex

[29]https://www.dewa.gov.ae/en/customer/innovation/renewable-energy/mohammed-bin-rashid-al-maktoum-solar-park).

[30] Della Ceca, L., Michelletti, M., Freire, M., García, B., Piacentini, R. SO2 and aerosol evolution over the very clear atmosphere at the Argentinean Andes range sites of San Antonio de los Cobres and El Leoncito. In Proceedings of the 2nd Int. Electron. Conf. Atmos. Sci., 16–31 July 2017. Sciforum Electronic Conference Series, Vol. 2, 2017.

[31]Margulis D. The photovoltaic solar generation and the saving in power that produce the technology (in Spanish). Energía estratégica, July 7, 2018 (available at: www.energiaestrategica.com/la-generacion-solar-fotovoltaica-y-los-ahorros-de-potencia-que-genera-la-tecnologia)

[32] IPCC (Intergovernmental Panel on Climate Change), Working Group I. "Climate change 2013: The physical science basis". Cambridge University Press, page 714, 2013b (also available at: www.ipcc.ch/pdf/assessmentreport/ar5/wg1/WG1AR5_Chapter08_FINAL.pdf).

[33] MEM (Ministerio de Energía y Minería de la Argentina). "Cálculo del factor de emisión 2015, de la Red Argentina de Energía Eléctrica", 2015 (available at: http://www.energia.gob.ar/contenidos/verpagina.php?idpagina=2311).